AlgSAT — a SAT Method for Search and Verification of Differential Characteristics from Algebraic Perspective

Huina Li[1,2], Guozhen Liu[2], Haochen Zhang[1], Kai Hu[2], Jian Guo[2] and Weidong Qiu[1]

[1] School of Cyber Science and Engineering, Shanghai Jiao Tong University, Shanghai, China

[2] Division of Mathematical Sciences, School of Physical and Mathematical Sciences, Nanyang Technological University, Singapore

Abstract. A good differential is a start for a successful differential attack. However, a differential might be invalid, *i.e.*, there is no right pair following the differential[1], due to some complicated contradictions that are hard to be considered. In this paper, we present a novel and handy method to search and verify a differential characteristic (DC) based on a recently proposed algebraic perspective on the differential(-linear) cryptanalysis (CRYPTO 2021).

From this algebraic perspective, exact Boolean expressions of differentials over a cryptographic primitive can be conveniently established, thus verifying a given DC is naturally a Boolean satisfiability problem (SAT problem). With this observation, our approach simulates the round function of the target cipher symbolically and derives a set of Boolean equations in Algebraic Normal Form (ANF). These Boolean equations can be solved by off-the-shelf SAT solvers such as `Bosphorus`, which accept ANFs as their input.

To demonstrate the power of our new tool, we apply it to Gimli, Ascon, and Xoodoo. For Gimli, we improve the efficiency of searching for a valid 8-round colliding DC compared with the previous MILP model (CRYPTO 2020). Our approach takes about one minute to find a valid 8-round DC, while the previous MILP model could not find any such DCs in practical time. Based on this DC, a practical semi-free-start collision attack on the intermediate 8-round Gimli-Hash is thus successfully mounted, *i.e.*, a colliding message pair is found. For Ascon, we check several DCs reported at FSE 2021. Firstly, we verify a 2-round DC used in the collision attack on Ascon-Hash by giving a right pair (such a right pair requires 2^{156} attempts to find in a random search). Secondly, a 4-round differential used in the forgery attack on Ascon-128's iteration phase is proven invalid, as a result, the corresponding forgery attack is invalid, too. For Xoodoo, we verify tens of thousands of 3-round DCs and two 4-round DCs extended from the so-called differential trail cores found by the designers or our search tool. We find all of these DCs are valid, which well demonstrates the sound independence of the differential propagation over Xoodoo's round functions. Besides, as an independent interest, we develop a SAT-based automatic search toolkit called XoodooSat to search for 2-, 3-, and 4-round differential trail cores of Xoodoo. Our toolkit finds two more 3-round differential trail cores of weight 48 that were missed by the designers which enhance the security analysis of Xoodoo.

Keywords: Cryptographic Permutation · SAT · Automatic Verification · Differential Characteristic Search · Semi-free-start Collision Attacks

[1] A differential can also be considered invalid when its actual probability is (significantly) different from the theoretically estimated one. Cases related to false probability are out of the scope of this paper.

1 Introduction

With the rapid development of the Internet of Things (IoT), more and more light mobile devices appear in people's daily life such as smart cards, wireless sensors, and Radio Frequency IDentification (RFID) tags. As these devices have limited memory and computing resources, it is infeasible to directly apply traditional encryption algorithms such as the Advanced Encryption Standard (AES) [DR02] in such scenarios. Therefore, lightweight cryptographic (LWC) algorithms have attracted more and more attention. Especially, in August 2018, the National Institute of Standards and Technology (NIST) initiated a competition [NIS18] to solicit, evaluate, and standardize LWC algorithms, including authenticated encryption with associated data (AEAD) and lightweight hash functions that are suitable for use in constrained environments. Three candidates, Gimli [BKL+19], Ascon [DEMS21], and Xoodyak [DHP+20] have attracted great attention because of their clean designs and high efficiency. On March 29, 2021, Ascon and Xoodyak were further announced as two of the ten finalist candidates of the competition.

Gimli, Ascon, and Xoodyak are all designed based on cryptographic permutations, which is an increasingly popular paradigm to design LWCs. These permutation-based ciphers usually bring high performances in both software and hardware implementations, but simultaneously their novel designs make cryptanalysts feel difficult to fully understand their security properties. As a result, always we would tend to study the security properties of the underlying permutations to deepen our understanding of the whole ciphers.

Similar to the classical block ciphers, these permutations are also iterated algorithms consisting of simple round functions. Naturally, some cryptanalytic methods originated for block ciphers have been borrowed to evaluate the security of permutations. One of the most important attacks among them is the differential cryptanalysis introduced by Biham and Shamir at CRYPTO 1990 [BS91]. In a differential attack, the attacker seeks a fixed input difference α_0 that propagates through a r-round primitive (the primitive could be a block cipher or a permutation) to a fixed output difference α_r with a high probability p, the differential is thus represented by (α_0, α_r). To find a proper differential (α_0, α_r) with a high probability for the primitive, we examine the differential property of the i-th $(1 \le i \le r)$ round and try to find a local differential for this round denoted by (a_{i-1}, a_i) whose probability is denoted by p_i. With a tacit assumption that differentials of two consecutive rounds are independent and its round subkeys (*resp.* round constants) are independent and uniformly random [LMM91], these local differentials for all rounds could be chained into one so-called differential characteristic (DC) $(\alpha_0, \alpha_1, \ldots, \alpha_r)$, whose probability is computed by $p = \prod_{i=1}^{r} p_i$. For the sake of simplicity, we generally refer to all these underlying assumptions as the Markov assumption in this paper.

With the Markov assumption, many methods such as the so-called automated tools have been invented to search for useful or even optimal DCs. When using the automated tools, the propagation rules of differentials for components of a primitive in each round are modeled by some specific constraints. All solutions satisfying these constraints are expectedly valid DCs. Based on these constraints, additional constraints like describing whether the corresponding Sboxes in the DCs are active or not would also be added to the constraint pool. The set formed by all these constraints is denoted by $\mathcal{C}$ in this paper. In general, a constraint representing the number of active Sboxes which is the so-called *objective function* and denoted by $\mathcal{O}$ is also imposed. Different automated tools handle $(\mathcal{C}, \mathcal{O})$ differently. There are three kinds of automated tools in the literature that are often used for the search: (a) the Boolean satisfiability problem (SAT) [MP13], where the constraints in $\mathcal{C}$ and the objective function are modeled by the corresponding clausal normal forms (CNFs) or algebraic normal forms (ANFs). An extension of the SAT called satisfiability modulo theories (SMT) [GD07] is also available which generalizes the SAT to more complex formulas involving *e.g.*, the integers and/or bit vectors. (b) the Mixed Integer Linear Programming (MILP) [MWGP11] where $(\mathcal{C}, \mathcal{O})$ are described by a set of inequalities (including equations). (c) the constraint programming (CP) [GMS16], where users could use more flexible formulas to describe $(\mathcal{C}, \mathcal{O})$. After generating $(\mathcal{C}, \mathcal{O})$ which is also called a model of the corresponding tools, we can delegate the most laborious part of searching for a DC to automatic tools.

Although the Markov assumption is generally considered reasonable for block ciphers, unfortunately, sometimes it would not hold for some permutations. At CRYPTO 2020 [LIM20], Liu, Isobe, and Meier pointed out that the 6-round and 2-round DC used for attacking Gimli-Hash and Ascon-Hash respectively found by MILP in [ZDW19] is invalid. In addition, a 12-round DC for Gimli permutation given by the designers [BKL+17] is also proved incompatible. That means, although these DCs seem legal under the Markov assumption, no conforming right pairs (pairs that propagate following the predefined DC) can be found in practical cryptanalysis. No sophisticated key schedule algorithms or round subkeys are considered as one of the reasons resulting in these incompatibilities.

In [LIM20], in order to make sure there is at least one conforming right pair following the DC, Liu *et al.* constructed an improved MILP model that considers simultaneously both the propagations of a DC $(\alpha_0, \alpha_1, \ldots, \alpha_r)$ and message pair $(x_0, x_1, \ldots, x_r)$ where x_i, $1 \leq i \leq r$, is the input into the i-th round function. By carefully analyzing the relations between α_i and x_i, their MILP model traces the hybrid path $((\alpha_0, x_0), (\alpha_1, x_1), \ldots, (\alpha_r, x_r))$. Therefore, if the MILP model is feasible, the solution will be a valid DC with a right pair. Later, Sadeghi, Rijmen, and Bagheri proposed another MILP model to verify a differential [SRB21]. Different from Liu *et al.*'s model that traces the difference and value, Sadeghi *et al.*'s approach directly traces the two encrypted values as $((x_0, x_0'), (x_1, x_1'), \ldots, (x_r, x_r'))$ and assigns the input and output differences as $\alpha_0 = x_0 \oplus x_0'$, $\alpha_r = x_r \oplus x_r'$ for the differential (α_0, α_r).

Both methods require analyses of different components of primitives to construct the inequalities, which is required us construct different model, such as AND-model, XOR-model. For example, Liu *et al.*'s model requires independently constructing three constraint models including a difference and value transitions model and a connection model which is used to describe the relations between difference and value in the non-linear layer, while Sadeghi *et al.*'s model constructs two values transitions model at the same time, and add some linear constraints to ensure that the XOR of two values transitions satisfy the given DC.

Although these methods directly constructing MILP model are very natural and simple, which cannot exploit the algebra of polynomials naturally. As the underlying permutation for most of LWC algorithms has a low algebraic degree of round function, it is natural for us to combine related algebraic techniques. To fill the gap in the security analysis of cryptographic permutations with low degree function, we propose a novel and efficient search and verification approach from an algebraic perspective inspired by the previous work of Liu, Lu and Lin [LLL21].

At CRYPTO 2021, Liu, Lu and Lin proposed an algebraic perspective on differential(-linear) cryptanalysis [LLL21]. This new algebraic perspective pointed out that the output difference of a Boolean function is a special Boolean function of the input difference and input value.

For a Boolean function $f : \mathbb{F}_2^n \to \mathbb{F}_2$ representing a certain output bit of a primitive, the output difference of f with respect to the input difference Δ at a point X is

$$\mathcal{D}_\Delta f(X) = f(X) \oplus f(X \oplus \Delta).$$

Liu *et al.* defined a new Boolean function f_Δ as

$$f_\Delta(X, x) = f(X \oplus x\Delta),$$

where x is an auxiliary binary variable. Then Liu *et al.* gave the following formula

$$\mathcal{D}_x f_\Delta = D_\Delta f, \tag{1}$$

where $\mathcal{D}_x f_\Delta$ is the partial derivative of f_Δ with respect to x. In this paper, we will directly build our approach based on Equation 1.

Our contributions. In this paper, the contributions are four-fold as follows,

A new method to search and verify a differential or DC.

According to Equation 1, the output difference of a Boolean function can be represented as a Boolean expression $\mathcal{D}_x f(X \oplus x\Delta)$, meaning that once the input difference Δ is fixed the output difference is completely determined by X. Therefore, to check whether $\mathcal{D}_x f(X \oplus x\Delta) = o \in \mathbb{F}_2$ holds equals to determine whether a solution X exists for this Boolean equation. In addition, if the input value X and output difference o are set free (*i.e.*, we do not specify their values), any solution (X, Δ, o) satisfying $\mathcal{D}_x f(X \oplus x\Delta) = o$ is a valid differential with a right pair $(X, X \oplus \Delta)$. Both of them are SAT problems that can be solved with many off-the-shelf SAT solvers. To construct the Boolean equation, we only need to simulate the update of the target cipher to obtain the expression of $\mathcal{D}_x f(X \oplus x\Delta)$, which is easy to handle by symbolic computation. In this paper, we take `SageMath` [The22] as the symbolic computation tool and the `Bosphorus` [CSCM19] as the SAT solver.

Applications to Gimli. For Gimli [BKL+19], Liu *et al.* used their MILP model to search for a valid 6-round Semi-Free-Start (SFS) collision DC according to the pattern in [ZDW19], which took them about 4 hours. As a comparison, it takes us only 24.11 seconds to provide a colliding DC and a right pair that satisfies the same DC pattern. In order to establish a SFS collision attack on the intermediate 8-round Gimli-Hash, the authors of [LIM20] proposed a conditional 8-round DC whose input and output differences are both active only in the rate part. Expectedly it requires 2^{64} attempts to find out such a DC satisfying all conditions if we search for it randomly. Liu *et al.* applied their MILP model to this problem trying to find a desirable right pair. Unfortunately, no solutions were returned in practical time [LIM20]. We apply our tool to this problem, and it shows that our tool is more efficient than their MILP model. In practice, it takes about one minute to find a colliding DC as well as a right pair that satisfies all those conditions. With this pair, we successfully mount a practical SFS collision attack on the intermediate 8-round Gimli-Hash. These collision message pairs are provided in this paper.

Applications to Ascon. For Ascon [GPT21], we examine some differentials proposed in previous forgery and collision attacks on Ascon-AEAD and Ascon-Hash. A 2-round DC that was used in the improved 2-round collision attack on Ascon-Hash, four 3-round DCs and a 4-round DC used in the forgery attacks on the finalization or iteration phases of Ascon-128 or Ascon-128A [GPT21] as well as a 5-round truncated DC in [DEMS21] are all proved valid. Namely, corresponding confirming right pairs are found for them.

On the other hand, a 4-round differential leveraged in the forgery attack on Ascon-128 reported in [GPT21] is found invalid since our tool proves no right pair exists. Thus, this forgery attack is accordingly invalid.

Applications to Xoodoo. For Xoodoo [DHAK18], the designers have exhaustively searched all 3-round *differential trail cores* up to weight[2] 50 with a dedicated tree search algorithm, among which the weight of optimal trail cores is 36. Each differential trail core actually corresponds to exponentially many real 3-round DCs expanded by the omitted χ operation. To examine the validity of these 3-round DCs, we randomly select tens of thousands of 3-round DCs extended from the differential trail cores, and we find all of them are valid, which demonstrates the sound independence of round functions of Xoodoo. Moreover, we also verify two 4-round DCs of weight 80 extended from two 4-round differential trail cores of weight 80[3] (found with our independent SAT-based automatic search toolkit called XoodooSat) by presenting their right pairs. As an independent interest,

[2]The *weight* of the differential trail cores is equal to $log_2(p^{-1})$, where p is the differential probability

[3]Recently, one paper [DMA22] that proves that the minimum weight of any 4-round trail core is 80 appeared in the ePrint.

Table 1: Comparison of our solving times with previous works.

Primitive	Rnd	In Attack	DC from	Validity	Our Time	Pre. Time
GIMLI-Hash	6	SFS collision	Tab.7	Valid	9.74s	4h [LIM20]
	8	SFS collision	Tab.9	Valid	66.71s	-† [LIM20]
ASCON-Hash	2	Collision	[GPT21]	Valid	0.02s	-
ASCON-128A	3	Forgery(final.)	[GPT21]	Valid	0.07s	-
	3	Forgery(iter.)	[GPT21]	Valid	0.31s	-
ASCON-128	3	Forgery(final.)	[GPT21]	Valid	0.08s	-
	3	Forgery(iter.)	[GPT21]	Valid	81s	-
	4	Forgery(final.)	[GPT21]	Valid	194s	-
	4	Forgery(iter.)	[GPT21]	Invalid	0.05s	-
	5	-	[DEMS21]	Valid	3894s	-
XOODOO	3	-	Tab.27	Valid	1.37s	-
	3	-	Tab.31	Valid	1.62s	-
	3	-	Tab.33	Valid	1.08s	-
	3	-	Tab.29	Valid	0.12s	-
	4	-	Tab.35	Valid	1.24s	-
	4	-	Tab.37	Valid	343s	-
KECCAK-f[800]	4	Collision	[GLST22]	Valid	7.86s	79s‡[SRB21]
KECCAK-f[1600]	4	Collision	[GLST22]	Valid	21.59s	210s‡[SRB21]

†The MILP model in [LIM20] could not return any results in practical time.
‡Using the verification method of [SRB21] to automatically verify DCs but with the help of SAT.

our toolkit also finds two more 3-round differential trail cores than the designers' tool [DHAK21] which were missed due to a bug in their implementation[4].

It is interesting to note that for permutations of large state size like KECCAK-f, our approach still shows excellent performance. Considering the similarities between the XOODOO and KECCAK-f, we verify one 4-round DC [5] of KECCAK-f[1600] and one 4-round DC of KECCAK-f[800] in [GLST22] with the weight of 133 and 95, respectively, and confirm that all of them are valid.

We give a summary of the best times achieved to verify DCs over various cryptographic primitives in Table 1. Compared with the previous methods [LIM20, SRB21], our method is superior to previous methods [LIM20, SRB21] in both efficiency and effectiveness. To better compare our method with [SRB21], we construct a SAT model using the previous verification method of [SRB21] to verify 4-round DC of KECCAK-f[800] and KECCAK-f[800], the obviously better results are obtained than that using the verification method of [SRB21]. All of our solving times are solved by `CryptoMiniSat` solver (version 5.8.0). All experiments are conducted on a server with Inter(R) Xeon(R) CPU E5-4650 v3 @ 2.10GHz 12 Core, 65G RAM, and Ubuntu 18.04.5.

Paper outline. The rest of this paper is organized as follows. In Section 2, we give some concepts used in our work. We describe the full details of our verification and search approach in Section 3. We present the application of our approach on GIMLI in Section 5, on ASCON in Section 4 and on XOODOO in Section 6, respectively. Finally, we conclude our paper in Section 7. Details of experimental data, including the solving times, DCs, and right pairs are given in Appendix.

[4]We have confirmed this with the Keccak team, the designers of XOODOO. After fixing this bug, the Keccak team continued to search for more 3-round differential trail cores up to weight 52.

[5]Since these two 4-round DCs omit the nonlinear layer of the last round, we refer to them as 3.5-round DCs in our verification.

2 Preliminaries

In this section, we give some related terms and properties used in our work. We also review the previous methods for DCs verification.

2.1 Differential Cryptanalysis

In a differential attack, the attacker seeks a fixed input difference α_0 that propagates through an r-round primitive (the primitive could be a block cipher or a permutation) to a fixed output difference α_r with a high probability p, the differential is thus represented by (α_0, α_r).

If there exists an ordered pair $(x, x \oplus \alpha_0)$ satisfying $f(x) \oplus f(x \oplus \alpha_0) = \alpha_r$, then it is said to follow the differential (α_0, α_r). In this case, we call (α_0, α_r) a valid differential, and $(x, x \oplus \alpha_0)$ is called a right pair.

Usually, finding a differential and computing its probability is difficult, so we tend to study the differential properties of every round of the cipher. Let $f = f^{r-1} \circ f^{r-1} \circ \cdots \circ f^0$ be an r-round iterative cipher and α_i, α_{i+1} be the input and output difference of $f^i, 0 \leq i < r$. $(\alpha_0, \alpha_1, \ldots, \alpha_r)$ is called a DC of the cipher f. If there is a vector of variables $(x_0, x_1, \ldots, x_r)$ satisfying $f^i(x_i) \oplus f^i(x_i \oplus \alpha_i) = \alpha_{i+1}$ for all $0 \leq i < r$, we say $\{(x_0, x_1, \ldots, x_r), (x_0 \oplus \alpha_0, x_1 \oplus \alpha_1, \ldots, x_r \oplus \alpha_r)\}$ is a right pair following the DC.

Following the Markov cipher assumption [LMM91] where the round functions are treated as independent functions, a differential and a DC whose probabilities are larger than 0 are always valid if we can find at least one right pair for them. However, the independence of round functions might not always hold, especially for permutations without round keys. Some inner contradictions are difficult to be considered when searching for a differential or DC. That means some differential attacks on certain ciphers might be false since the differentials or DCs used in the attacks might be invalid. Therefore, it is necessary to check the validity of differentials or DCs of a permutation derived under the Markov assumption.

2.2 Algebraic Perspective on Differential(-Linear) Cryptanalysis

At CRYPTO 2021 [LLL21], Liu, Lu, and Lin presented a new algebraic perspective on differential cryptanalysis. As shown in Equation 1, the output difference of a Boolean function can be explicitly expressed as a Boolean expression. When applied to a cryptographic primitive with multiple output bits, each output bit can be represented by a Boolean function (expressed in ANF) of the input bits. Accordingly, the output difference of the primitive is determined by applying Equation 1 to all output bits.

Although theoretically Equation 1 is exact and requires no assumptions, the ANF of f_Δ as well as $\mathcal{D}_x f_\Delta$ in Equation 1 is difficult to obtain for a modern cryptographic primitive. To overcome the obstacle, Liu *et al.* introduced the differential algebraic transitional form (DATF) to obtain a simpler expression of $\mathcal{D}_x f_\Delta$ with variable substitutions.

Consider a cryptographic primitive that consists of r rounds, *i.e.*, $E = E_{r-1} \circ E_{r-2} \circ \cdots \circ E_0$, where $E_i : \mathbb{F}_2^n \to \mathbb{F}_2^n, 0 \leq i < r$ are the i-th round function. Each coordinate of the output of E is viewed as a composite ANF. For a difference Δ and a value X, we study the differential property of E_0 first. According to Equation 1, we first compute $E_0(X \oplus x\Delta)$. Next we do variable substitutions for each output bit of $E_0(X \oplus x\Delta)$. Suppose f_i^0 is the i-th bit of its output, which could be uniquely written as $f_i^0 = (f_i^0)'' x \oplus (f^0)'$, where $(f_i^0)''$ and $(f^0)'$ are independent of x, we introduce two transitional variables a_i^0 and b_i^0 to substitute $(f_i^0)''$ and $(f^0)'$, respectively. Thus f_i^0 could be simplified in form to $f_i^0 = a_i^0 x \oplus b_i^0$. When the variable substitutions of all output bits of E_0 are finished, we could compute the output bits of E_1 based on the simplified expressions of E_0's output and do variable substitutions for E_1. Repeat this process until we derive a transitional form of the output of E. Note we retain x during the substitution process, thus a simplified expression of $\mathcal{D}_x f_\Delta$ can be derived in every step.

2.3 SAT-based Cryptanalysis

Given a Boolean formula $f(x_1, x_2, \ldots, x_n)$, the Boolean satisfiability problem (SAT) is to determine whether there is any assignment of values to these Boolean variables which makes the formula true. The SAT problem is satisfiable if a valid assignment exists, otherwise it is unsatisfiable. Most of the previously introduced SAT-based cryptanalysis methods [SWW18, SWW21, GLST22] encode directly the cryptanalysis problem as a SAT instance under the Markov assumption and then invoke the off-the-shelf SAT solver to solve it.

There are many off-the-shelf SAT solvers available which have been introduced into cryptanalysis, such as the `CryptoMiniSat` [SNC09] and `CaDiCaL` [Bie19]. Usually, modern SAT solvers based on *conflict-driven clause learning* (CDCL) [MLM21] support the CNF as their input which uniquely defines a Boolean formula. A formula in CNF consists of clauses joined by *conjunctions* ($\wedge$), where each clause is a *disjunction* ($\vee$) of *literals*, each literal represents a positive or negative variable, *e.g.*, x_i or $\neg x_i$.

However, for cryptanalysts, ANF which consists of $\oplus$ and $\wedge$ is more friendly and preferred to use since the output bits of a cryptographic primitive are naturally written as ANFs of its input bits. Unfortunately, compared with CNF solvers, ANF solvers on huge polynomial systems often use more memory that might be infeasible on many computing platforms.

To fill this vacancy, Davin *et al.* proposed an ANF simplification and solving tool, called `Bosphorus` [CSCM19], which bridges between ANF and CNF solving techniques. The `Bosphorus` supports the ANFs as its input, which could take advantage of the algebra of polynomials naturally. It first uses many optimized mathematical algorithms, including XL [CKPS00], Brickenstein's ANF-to-CNF conversion [BD09], Gauss-Jordan elimination, *etc.*, to simplify ANFs and converted these highly optimized ANFs to CNFs. Afterwards, the SAT solver `Cryptominisat` within `Bosphorus` is invoked to solve those CNFs. Hence, the `Bosphorus` can be roughly seen as a SAT solver that supports the ANFs as input.

2.4 Previous Automatic Verification of Differential Characteristics

To the best of our knowledge, there are two categories of methods based on automatic tools for verifying differentials or DCs. The main idea of the first one [LIM20, BM22] is to independently construct three constraint models including difference and value transitions and a connection model which is used to describe the relations between differences and values in the non-linear layer. In this way, a DC and the conforming message pair can be found simultaneously. In [LIM20], Liu *et al.* took the MILP to construct the constraint models while in [BM22], Bellini and Makarim leveraged the SMT.

The second method [MZ06, HLJ+20, SRB21] directly traces the two encrypted values which follow a fixed DC. In [SRB21], Sadeghi *et al.* tries to construct the MILP model of two value transitions at the same time, and add some linear constraints to ensure that the XOR of two value transitions satisfies the given differential characteristic $(\Delta Y_0, \Delta Y_1, \ldots, \Delta Y_n)$. Once the solution is feasible the given DC is valid. This idea has already been used by [MZ06] to trace two input states that satisfy a fixed DC, which is the critical step to finding a collision of the hash function. A similar strategy was ever applied in searching the impossible differentials and impossible $(s+1)$-polytopic transitions by Hu *et al.* [HLJ+20].

Both methods based on the MILP/SMT/SAT tools are natural and simple for most cryptographic primitives. More work is focused on encoding cryptanalysis problems manually in inequalities/CNF forms, including modeling the nonlinear operation of target primitives, such as the AND-model, OR-model, and S-box model. However, it is slightly time-consuming to re-construct the model if one has a different representation of the primitive. Moreover, the previous two methods cannot take advantage of the algebraic properties of constraints, which maybe decrease the efficiency in terms of the model-solving stage. In this paper, we aim at filling the gap in the search and verification of cryptographic permutation. The results show our approach is more handy and efficient listed in Table 1.

3 Verification of a Differential or Differential Characteristic from Algebraic Perspective

In this section, based on Liu et al.'s differential cryptanalysis from an algebraic perspective [LLL21], we introduce a new approach to efficiently verify a differential or DC as well as directly find a valid DC. The basic idea is to transform Equation 1 into a SAT problem which is handy to solve by SAT solvers.

3.1 SAT Model for Verifying a Differential or Differential Characteristic

Given a cryptographic primitive $E : \mathbb{F}_2^n \to \mathbb{F}_2^n$, we denote its n output bits as n ANFs by $(f_0, f_1, \ldots, f_{n-1})$. We introduce our novel method of verifying a differential in two cases according to whether the ANFs of output bits of E are available.

Simple case. In the simple case, suppose we can derive the ANFs of all output bits of E. According to Equation 1, to verify a given differential $(\Delta, \nabla) \in \mathbb{F}_2^n \times \mathbb{F}_2^n$, we need to compute the ANFs of $(f_0(X \oplus x\Delta), f_1(X \oplus x\Delta), \ldots, f_{n-1}(X \oplus x\Delta))$. The output difference $\nabla = (\nabla_0, \nabla_1, \ldots, \nabla_{n-1}) \in \mathbb{F}_2^n$ is thus $(\mathcal{D}_x f_0(X \oplus x\Delta), \mathcal{D}_x f_1(X \oplus x\Delta), \ldots, \mathcal{D}_x f_{n-1}(X \oplus x\Delta))$. Verifying the differential (Δ, ∇) is equivalent to checking if the following equation set is solvable.

$$\begin{cases} \nabla_0 = \mathcal{D}_x f_0(X \oplus x\Delta) \\ \nabla_1 = \mathcal{D}_x f_1(X \oplus x\Delta) \\ \quad\vdots \\ \nabla_{n-1} = \mathcal{D}_x f_{n-1}(X \oplus x\Delta) \end{cases} \tag{2}$$

Note that $\mathcal{D}_x f_i(X \oplus x\Delta)$, where $0 \leq i < n - r$, are the ANFs of X. Equation 2 is naturally a SAT problem that can be solved with a SAT solver.

Example 1. Take the 5-bit Sbox of Ascon as an example (the ANFs of the Sbox is presented later in Equation 6 in Section 4.1). Let the input value be $X = (x_0, x_1, x_2, x_3, x_4)$ and the ANFs of the output bits are denoted by $(f_0, f_1, f_2, f_3, f_4)$. To verify whether (Δ, ∇) is a valid differential where $\Delta = (1, 1, 1, 0, 0)$ and $\nabla = (1, 0, 0, 0, 0)$, $X \oplus x\Delta = (x_0 \oplus x, x_1 \oplus x, x_2 \oplus x, x_3, x_4)$, we compute the expressions of the 5-bit output difference according to Equation 2 as follows.

$$\begin{cases} D_x f_0(X \oplus x\Delta) = x_0 \oplus x_2 \oplus x_4 \oplus 1 \\ D_x f_1(X \oplus x\Delta) = x_1 \oplus x_2 \\ D_x f_2(X \oplus x\Delta) = 0 \\ D_x f_3(X \oplus x\Delta) = x_3 \oplus x_4 \oplus 1 \\ D_x f_4(X \oplus x\Delta) = x_0 \oplus x_1 \oplus x_4 \end{cases}$$

Since the output difference is $\nabla = (1, 0, 0, 0, 0)$, we obtain the following five equations.

$$\begin{cases} x_0 \oplus x_2 \oplus x_4 \oplus 1 = 1 \\ x_1 \oplus x_2 = 0 \\ 0 = 0 \\ x_3 \oplus x_4 \oplus 1 = 0 \\ x_0 \oplus x_1 \oplus x_4 = 0 \end{cases}$$

In Example 1, the five equations are easy to solve even by hand. But most of the time, the equations are much more complicated. We regard them as a SAT problem and use `Bosphorus` to solve these ANFs to decide whether (Δ, ∇) is valid or not by observing whether a solution $(x_0, x_1, x_2, x_3, x_4)$ would be returned.

Complicated case. If the state size of a cryptographic primitive is large, it is computationally infeasible to compute the exact ANFs of the output bits. Inspired by the DATF technique [LLL21], we take advantage of the variable substitutions to simplify the form of the ANFs while retaining the variable x. Suppose E consists of $E = E_{r-1} \circ \cdots \circ E_1 \circ E_0$ where the ANFs of E_i are available, and the output bits of E_i is denoted by $(f_0^{i+1}, f_1^{i+1}, \ldots, f_{n-1}^{i+1})$. To verify a differential (Δ, ∇), we first focus on E_0 and compute the ANFs of $(f_0^1(X \oplus x\Delta), f_1^1(X \oplus x\Delta), \ldots, f_{n-1}^1(X \oplus x\Delta))$. Subsequently, we introduce $2n$ transitional variables a_j^1, b_j^1, where $0 \le j < n$ to perform the variable substitutions as follows.

$$\begin{cases} f_j^1(X \oplus x\Delta) = b_j^1 \oplus a_j^1 x \\ a_j^1 = \mathcal{D}_x f_j^1(X \oplus x\Delta) \\ b_j^1 = \mathcal{D}_x f_j^1(X \oplus x\Delta)x \oplus f_j^1(X \oplus x\Delta) \end{cases}, \; 0 \le j < n \tag{3}$$

Based on Equation 3 (which are the ANFs of transitional variables a^1, b^1 and x), we compute the outputs of E_1, *i.e.*, perform similar variable substitutions by introducing $2n$ new transitional variables $a_j^2, b_j^2, 0 \le j < n$.

$$\begin{cases} f_j^2(b^1 \oplus a^1 x) = b_j^2 \oplus a_j^2 x \\ a_j^2 = \mathcal{D}_x f_j^2(b^1 \oplus a^1 x) \\ b_j^2 = \mathcal{D}_x f_j^2(b^1 \oplus a^1 x)x \oplus f_j^2(b^1 \oplus a^1 x) \end{cases}, \; 0 \le j < n \tag{4}$$

Note that we omit the subscript of a_j^1 and b_j^1 in Equation 4 for simplicity. Repeat this process until the simplified forms of the ANFs of

$$(f_0^r(b^{r-1} \oplus a^{r-1}x), f_1^r(b^{r-1} \oplus a^{r-1}x), \ldots, f_{n-1}^r(b^{r-1} \oplus a^{r-1}x)) \tag{5}$$

is obtained. Likewise, we omit the subscript of f_j^r, and write Equation 5 as $f^r(b^{r-1} \oplus a^{r-1}x)$. Finally, we add constraints on the overall output difference $\nabla = (\nabla_0, \nabla_1, \ldots, \nabla_{n-1})$ with

$$\mathcal{D}_x f_j^r(b^{r-1} \oplus a^{r-1}x) = \nabla_j, 0 \le j < n.$$

In this way, we get a set of ANFs that determines whether (Δ, ∇) is a valid differential. Obviously, it is also a SAT problem.

Verifying a differential characteristic or differential. It is easy to adapt the above verification process for a differential or an r-round DC $(\Delta^0, \Delta^1, \ldots, \Delta^r)$ where $\Delta^i, 0 < i \le r$ is the output difference of the $(i-1)$-th round and Δ^0 is the initial input difference. When the output ANFs of the i-th round are obtained and the variable substitutions are finished, extra constraints (as shown in the following) are added to the model to verify a DC.

$$\mathcal{D}_x f_j^i = \Delta_j^i$$

Algorithm 1 Verification of Differential Characteristics

Require: An unknown message $X = (x_0, \ldots, x_{n-1})$, the primitive $E = E_{r-1} \circ \cdots \circ E_0$, the number r of rounds, a given DC $(\Delta^0, \Delta^1, \ldots, \Delta^r)$, an auxiliary binary variable x.
Ensure: The value of X or "Invalid".

Initialize the input variable vector $f^0 = X \oplus x\Delta^0$ and allocate a set $Q = \emptyset$;
for i from 0 to $r - 1$ **do**
    Compute the output of E_i according to the ANF of E_i , $f^{i+1} \leftarrow E_i(f^i)$
    Add $\mathcal{D}_x f^{i+1} = \Delta^{i+1}$ to Q ▷ For verifying a differential, only when $i = r - 1$ we execute this step
    Introduce transitional variables a^{i+1}, b^{i+1}, let $f^{i+1} = a^{i+1}x \oplus b^{i+1}$ ▷ The substitution rule is used after the nonlinear operations by default.
    Add $a^{i+1} = \mathcal{D}_x f^{i+1}$ and $b^{i+1} = \mathcal{D}_x f^{i+1} x \oplus f^{i+1}$ to Q
end for
ANF optimization stage: simplify Q by invoking *anfread*() and perform ANF-to-CNF using *cnfwrite*() in `Bosphorus`;
SAT solving stage: solve CNFs using *solvewrite*() in `Bosphorus`, or using other modern SAT solver;
if The SAT problem is feasible **then**
    return X
else
    return "Invalid"
end if

Similarly, by ignoring the ANFs of intermediate difference, we verify the validity of a differential that utilizes a differential (Δ^0, Δ^r) rather than a specific DC. The process that verifies a DC or a differential is illustrated in Figure 1 and Algorithm 1.

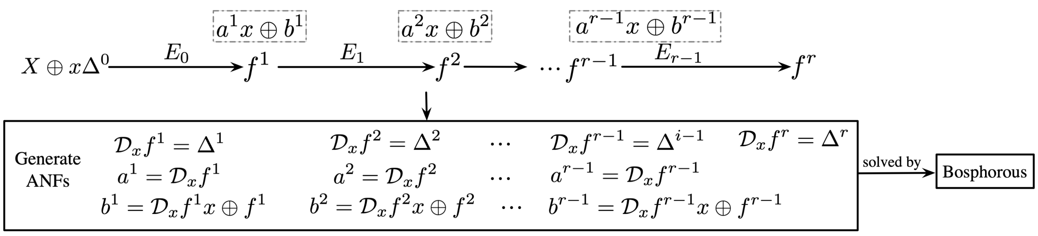

Figure 1: The illustration of our verification method

Searching for valid differential characteristics. In addition to verifying a given differential (Δ, ∇) or a DC $(\Delta^0, \Delta^1, \ldots, \Delta^r)$, our method can also be directly applied to search for valid DCs and the conforming message pair simultaneously. The only distinction is that we do not add constraints on ∇ or $\Delta^i, i \geq 1$ and let these unknown differences be free variables. On the other hand, if values of some inner variables are given in advance, *e.g.*, when we are dealing with a conditional DC, we can fix those variables accordingly as additional constraints. In this way, every solution to the SAT problem is a valid DC and a conforming message pair.

This method is especially useful for scenarios where DCs of a specific form such as the collision DCs used in collision attacks.

3.2 Obtaining and Solving the SAT Model

We exploit `SageMath` [The22] to obtain the ANFs of the output bits of a cipher. `SageMath` is a popular tool in cryptanalysis that has been used in some previous papers. For example, in [SHW+14], Sun *et al.* took `SageMath` to generate inequalities for a convex hull. `SageMath` also offers good support for calculating Boolean equations (represented by ANFs) over a ring and field. By simulating the round functions of the target cipher with variable substitutions, a set of ANFs linking the input and output differences are established.

Rather than solve the set of ANFs straightforwardly, we first simplify them with a simplification tool called `Bosphorus`. Our experiments show that the `Bosphorus` simplifies the set of ANFs significantly and returns a smaller as well as compact SAT model in CNFs. A detailed comparison of ANF size before and after optimization is provided in Appendix A. It's interesting to note that `Bosphorus` can even detect some contradictions among the ANFs set directly. If any contradictions happen, it will return UNSAT. After simplification and conversion, the `Cryptominisat` which is embedded in the `Bosphorus` will be invoked to solve the set of CNFs. Finally, we observe the returned solution to the SAT problem. If there is no solution, the target differential or DC is invalid, and some contradictions happen in the propagation; otherwise, a confirming right pair will be derived.

Moreover, in this paper, `CryptoMiniSat` shows outstanding performance in SAT solving with multi threads, compared with `CaDiCaL`. We solve the final CNFs using `CryptoMiniSat` and `CaDiCaL` solver. Our results show that the `CryptoMiniSat` has higher efficiency in terms of verifying DCs than `CaDiCaL`. The solving times of the two solvers are given in Appendix A.

3.3 Discussion on Our New Verification Algorithm

Similar to the previous verification algorithms such as [LIM20], our new verification algorithm also traces the propagation of both the values and differences over the target primitive. However, there are some essential differences between our new verification algorithms and [LIM20].

Firstly, the relations between the value transitions and difference transitions are very different. The verification algorithm in [LIM20] manually derived the relations between the values and differences for the nonlinear functions (the difference transitions and value transitions are dependent only on the nonlinear operation). For example, to the nonlinear functions of Gimli, the authors of [LIM20] derived four types of Boolean relations between the value and difference transitions. More importantly, their manual analysis is not universal, for different cryptographic primitives we need to analyze their nonlinear operations separately,such as S-boxes. Instead, the fundamental theory of our algorithm is the algebraic perspective of differential cryptanalysis proposed recently in [LLL21]. Thanks to the new perspective, the Boolean expressions of the output difference of a cryptographic primitive can be explicitly presented. As has been shown in Section 3.1, after setting the initial input of the primitive (*i.e.*, the input is $X \oplus x\Delta$), we do not need to care about the relations between the values and differences over any operation in the process. All we need to do is to simulate the update function by symbolic computations which is friendly to almost all kinds of cryptographic primitives.

Secondly, both our algorithm and [LIM20] try to find a solution for a target differential or DC rather than prove something is optimal. Unlike their transformation of the relation into a MILP problem[6], in our algorithm, we choose to use SAT to solve this problem from scratch. Fortunately, the relations derived from our algorithm are an inherited SAT model with ANF forms. By invoking the `Bosphorus`, we can directly simplify and solve this SAT model. As a result, we find the efficiency of our algorithm is significantly higher than

[6]Actually, their model can also be transformed into a SAT problem with extra works.

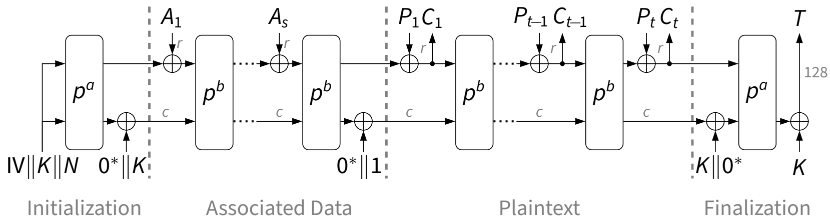

(a) Ascon-AEAD scheme

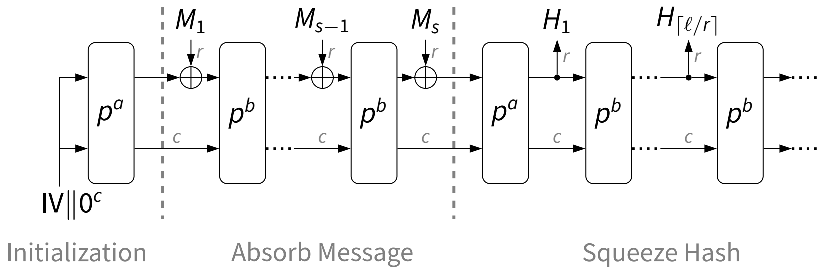

(b) Ascon-Hash scheme

Figure 2: The illustration of Ascon-AEAD and Ascon-Hash schemes.

[LIM20]. For example, Liu *et al.* used their MILP model to search for a valid 6-round SFS collision DC according to a pattern in [ZDW19], this cost them about 4 hours. Our verification algorithm is more efficient since it took only 9.74 seconds to find a valid DC. Besides, one 8-round SFS colliding DC and the conforming colliding pair was obtained in only 66.71 seconds using our algorithm, while any of such DCs could not be found by [LIM20] in practical time.

4 Application to Ascon

4.1 A Brief Introduction to Ascon

Ascon [DEMS21] has been announced by NIST as one of ten finalists in the lightweight cryptography standardization competition. The Ascon family consists of AEAD and Hash schemes. Ascon-AEAD adopts a MonkeyDuplex [BDPA11] mode with a stronger keyed initialization and keyed finalization phases as illustrated in Figure 2a. Ascon-Hash takes a sponge structure [BDPVA07] and the compressing process is shown in Figure 2b[7]. Both schemes operate on a state of 320 bits which they update with two permutations p^a and p^b whose rounds are respectively a and b. The 320-bit state S is divided into a r-bit rate part and a c-bit capacity part. The underlying permutations p^a and p^b are iterative designs and consists of three simple steps p_C, p_S, and p_L, denoted by $p = p_L \circ p_S \circ p_C$.

The round function p operates on a 320-bit state S arranged into five rows, *i.e.*, $S = w_0\|w_1\|w_2\|w_3\|w_4$, each row is a 64-bit register word. In internal convention, the bits of each 64-bit word are denoted by $S[64i + k], 0 \leq i < 5, 0 \leq k < 64$, where i is the index of row, $S[\frac{64i+k}{8}]$ indicates the most significant bit (MSB) of a byte.

Addition of Constants (p_C). p_C adds a round constant c_i to register word w_2 of the state S in round i. The round constants c_i is shown in Table 2.

Substitution Layer (p_S). p_S operates the state S with 64 parallel applications of the 5-bit Sbox to each bit-slice of the five registers w_0, w_1, w_2, w_3, w_4. We suppose the input

[7]These two figures for Ascon-AEAD and Ascon-Hash are borrowed from Ascon's website https://ascon.iaik.tugraz.at.

Table 2: Constants c_i used in the Ascon Permutation

Round i	Constant c_i	Round i	Constant c_i
0	00000000000000000f0	6	0000000000000000096
1	00000000000000000e1	7	0000000000000000087
2	00000000000000000d2	8	0000000000000000078
3	00000000000000000c3	9	0000000000000000069
4	00000000000000000b4	10	000000000000000005a
5	00000000000000000a5	11	000000000000000004b

of single 5-bit Sbox is $(x_0, x_1, x_2, x_3, x_4)$, and the output is $(y_0, y_1, y_2, y_3, y_4)$. The ANF of the single Sbox is given by

$$\begin{aligned} y_0 &= x_4x_1 \oplus x_3 \oplus x_2x_1 \oplus x_2 \oplus x_1x_0 \oplus x_1 \oplus x_0 \\ y_1 &= x_4 \oplus x_3x_2 \oplus x_3x_1 \oplus x_3 \oplus x_2x_1 \oplus x_2 \oplus x_1 \oplus x_0 \\ y_2 &= x_4x_3 \oplus x_4 \oplus x_2 \oplus x_1 \oplus 1 \\ y_3 &= x_4x_0 \oplus x_4 \oplus x_3x_0 \oplus x_3 \oplus x_2 \oplus x_1 \oplus x_0 \\ y_4 &= x_4x_1 \oplus x_4 \oplus x_3 \oplus x_1x_0 \oplus x_1 \end{aligned} \tag{6}$$

Linear Diffusion Layer (p_L). p_L provides diffusion within each 64-bit register word $w_i, 0 \leq i < 5$ as follows,

$$\begin{aligned} w_0 &\leftarrow \Sigma_0(w_0) = w_0 \oplus (w_0 \ggg 19) \oplus (w_0 \ggg 28) \\ w_1 &\leftarrow \Sigma_1(w_1) = w_1 \oplus (w_1 \ggg 61) \oplus (w_1 \ggg 39) \\ w_2 &\leftarrow \Sigma_2(w_2) = w_2 \oplus (w_2 \ggg 1) \oplus (w_2 \ggg 6) \\ w_3 &\leftarrow \Sigma_3(w_3) = w_3 \oplus (w_3 \ggg 10) \oplus (w_3 \ggg 17) \\ w_4 &\leftarrow \Sigma_4(w_4) = w_4 \oplus (w_4 \ggg 7) \oplus (w_4 \ggg 41) \end{aligned}$$

Moreover, an r-round DC of Ascon permutation $(\beta_0, \alpha_1, \beta_1, \ldots, \alpha_r)$ is represented as the following form

$$\beta_0 \xrightarrow{p_S \circ p_C} \alpha_1 \xrightarrow{p_L} \beta_1 \xrightarrow{p_S \circ p_C} \alpha_2 \xrightarrow{p_L} \cdots \xrightarrow{p_S \circ p_C} \alpha_r, \tag{7}$$

where β_i is the input difference of i-th $p_S \circ p_C$, α_{i+1} is the output difference of the i-th p_S, $0 \leq i < r$, and $\beta_i[j]$ is the j-th bit of $\beta_i, 0 \leq j < 320$.

4.2 Verification of the DCs in Forgery and Collision attacks

In this section, we show how to leverage our verification method introduced in Section 3 to verify some differentials or DCs proposed in previous forgery and collision attacks on Ascon-AEAD and Ascon-Hash, respectively.

Nonexistence of a category of DCs for 2-round Ascon-Hash in [ZDW19]. In [ZDW19], a 2-round collision attack on Ascon-Hash was proposed that is based on a 2-round DC. In order to construct this DC, they firstly found a 1-round DC (β_1, β_2) with the output difference β_2 active only in the rate part. Then, they used the target differential algorithm (TDA) [DDS12] to link this DC to the initial state of the internal permutation. In this way, they derived a 2-round DC $(\beta_0, \beta_1, \beta_2)$ and its input difference β_0 is nonzero only in the rate part. Unfortunately, this DC was proved invalid by [LIM20].

In this paper, we are interested in whether we can find an alternative and valid DC which satisfies the setting of [ZDW19] which the capacity parts of both the input and output differences be zero, with the same output difference β_2.

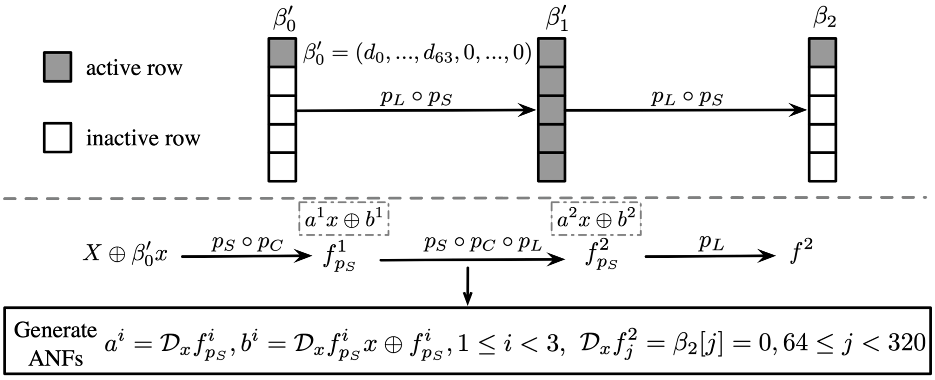

Figure 3: Our search and verification process

First of all, we fix the capacity part of the input difference β'_0 to be zero and let its 64-bit rate part be free variables. The input of the 2-round Ascon is set as $X \oplus \beta'_0 x$, where $X = (x_0, x_1, \cdots, x_{319})$ is a 320 binary variable representing one value of the input message, x is an auxiliary Boolean variable. Next, we compute the intermediate states including the first p_S denoted by $f^1_{p_S}$ and the output state of the first round and second round, denoted by f^1 and f^2, respectively. Figure 3 shows the detailed search and verification process.

Under these conditions, we take `SageMath` to obtain all corresponding ANFs and the verification problem is converted to a SAT problem. Finally, we invoke `Bosphorus` to solve this SAT problem, the result shows this SAT model was infeasible, which means all 2-round DCs satisfying the above restrictions do not exist.

Verify a DC for 2-round Ascon-Hash in [GPT21]. In [GPT21], Gerault, Peyrin, and Tan used the CP tool to find a new 2-round DC which also could be used in collision attack on 2-round Ascon-Hash. Since the DC proposed in [ZDW19] has been proved invalid, a similar case may also happen to this DC. Therefore, it is necessary to check its validity of it.

With the `SageMath`, the SAT model is constructed easily based on Algorithm 1. A right pair following this DC is returned in less than one second, this right pair is presented in Table 11. Therefore, we confirm that this characteristic is valid. Note the probability of this DC is 2^{-156}, so it requires 2^{156} tempts to search for the right pair in a random setting.

Check the differential and DCs in forgery attacks on Ascon-128 and Ascon-128A. In [GPT21], the authors proposed several forgery attacks against the finalization as well as the iteration phases of Ascon-AEAD. Firstly, they constructed a CP model to search for forgery DCs with different constraints for different phases. These forgery DCs can be found in Appendix C of this paper. Using these DCs, they improved the forgery attacks against the finalization phase of 3-round Ascon-128 as well as the iteration phase of 3-round Ascon-128A. Again, we need to check these DCs to see whether they are valid.

We apply Algorithm 1 to these forgery DCs. For forgery attacks against the finalization phase of 3-round Ascon-128 and Ascon-128A (see Table 16 and Table 12) and 4-round Ascon-128 in Table 21, we prove that all of these DCs are valid. The corresponding right pairs are given in Tables 17, Table 13 and Table 22. For forgery attacks against the iteration phase of 3-round Ascon-128 and Ascon-128A (see Table 18 and Table 14), we confirm that this characteristic is valid too and the corresponding conforming right pairs are shown in Tables 19 and 15.

In addition, we apply our algorithm to check the 4-round forgery DC in the iteration phase (see Table 20), and our program immediately returns "Invalid". That means this 4-round DC is invalid. We are interested in what results in its invalidity. To find the contradictions hidden among the DC and message value, we separate the whole 4-round

DC into two parts (every part contains 2 rounds) and apply Algorithm 1 to both of them separately. In the first two rounds, we can obtain the right message pair, but in the second two rounds, our program immediately returns "Invalid" in less one second. Therefore, there are some contradictions hidden in the third and fourth rounds. We show why the 4-round forgery DC in the iteration phase is invalid in Section 4.3.

Finally, we are curious about whether the corresponding 4-round forgery differential (rather than the DC) is valid. To check it, we remove the restrictions on the internal differences while fixing the input and output difference and run our algorithm again. Surprisingly, the loose model is still "Invalid", which means this 4-round differential is impossible for any right pairs, *i.e.*, it is invalid.

5-round results. We verified one 6-round truncated collision-producing DC for Ascon-128 identified in [DEMS21]. However, we are not able to find any solution in a limited time (15 days). Therefore, we only checked the first 5 rounds of 6-round truncated DC. The result shows that `Bosphorus` can return a valid 5-round DC (see Table 23) and a conforming right pair (see Table 24) simultaneously in about one hour.

4.3 Explaining the Contradictions

In this section, we discuss about why the 4-round forgery DC in the iteration phase is invalid. To find the contradictions hidden among the DC and value, we separate the whole 4-round DC into two parts (every part contains 2 rounds) and apply Algorithm 1 to both of them separately. In the first two rounds, we can obtain the right message pair, but in the second two rounds, `Bosphorus` returns "UNSAT" immediately. Therefore, there are some contradictions hidden in the last two rounds.

Thanks to that `Bosphorus` could directly detect contradictions among our ANF sets so that we can find the reasons of the contradiction. For a better understanding of what causes the contradiction, we extract all the set ANFs of the last two rounds based on Algorithm 1. Denote the last two round DC by $(\beta_2, \alpha_3, \beta_3, \alpha_4)$, we could obtain the following set of ANFs, where $f_S^r[i]$ is the ANF of i-th output bit after the r-th nonlinear operation p_S:

$$\begin{cases} D_x f_S^3[i] = \alpha_3[i] \\ D_x f_S^4[i] = \alpha_4[i] \\ a_i^1 = D_x f_S^3[i] \\ b_i^1 = D_x f_S^3[i] x \oplus f_S^3[i] \\ x_{320+i} = a_i^1 \\ x_{640+i} = b_i^1 \end{cases}, 0 \leq i < 320 \tag{8}$$

The value of some bits of input state X and intermediate state b^1 can be deduced according to the ANFs of $D_x f_S^3[i] = \alpha_3[i]$ and $b_i^1 = D_x f_S^3[i] x \oplus f_S^3[i], 0 \leq i < 320$ which is displayed in Figure 4.

Moreover, we are able to get the simplified ANFs of $b_{664}^1 = D_x f_S^3[24] x \oplus f_S^3[24]$ and $b_{856}^1 = D_x f_S^3[216] x \oplus f_S^3[216]$ based on this figure,

$$\begin{cases} x_{24}x_{88} \oplus x_{24} \oplus x_{88}x_{152} \oplus x_{88}x_{280} \oplus x_{88} \oplus x_{152} \oplus x_{216} \oplus x_{664} = \boldsymbol{x_{152} \oplus x_{664} = 0} \\ x_{24}x_{216} \oplus x_{24}x_{280} \oplus x_{24} \oplus x_{88} \oplus x_{152} \oplus x_{216} \oplus x_{280} \oplus x_{856} = \boldsymbol{x_{152} \oplus x_{856} \oplus 1 = 0} \end{cases}$$

Based on the above conditions, we could explain one of the contradiction. A set of ANFs is extracted using $D_x f_S^4 = \alpha_4$ that leads to a contradiction as follows,

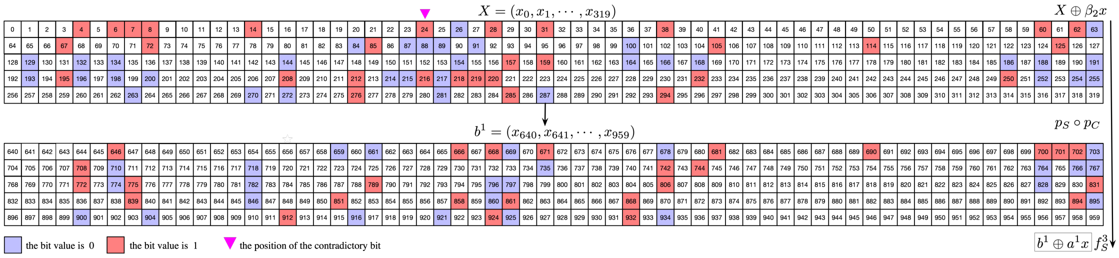

Figure 4: Propagation of input value before and after $p_S \circ p_C$

$$
\begin{cases}
\mathcal{D}_x f_S^4[216] = \alpha_4[216] = 0 \\
\mathcal{D}_x f_S^4[216] = x_{645} \oplus x_{664} \oplus x_{700} \oplus 1 \\
\mathcal{D}_x f_S^4[152] = \alpha_4[152] = 0 \\
\mathcal{D}_x f_S^4[152] = x_{839} \oplus x_{846} \oplus x_{856} \oplus 1 \\
\mathcal{D}_x f_S^4[197] = \alpha_4[197] = 0 \\
\mathcal{D}_x f_S^4[197] = x_{645} \oplus x_{681} \oplus x_{690}
\end{cases}
$$

Observe the above equation, if we set the 152-th bit of the input value, *i.e.*, x_{152} is 1, then x_{664} is 1 according to $x_{152} \oplus x_{664} = 0$, x_{645} is 1 computed using $\mathcal{D}_x f_S^4[216] \oplus x_{664} \oplus x_{700} \oplus 1$. However, $\mathcal{D}_x f_S^4[197]$, which is derived from our formula for the 197-th bit of the output difference can be calculated from $x_{645} \oplus x_{681} \oplus x_{690}$ and determine the value of $\mathcal{D}_x f_S^4[197]$ as 1. Therefore, there is a contradiction. On the other hand, if we set x_{152} is 0, then x_{856} is 1 according to $x_{152} \oplus x_{856} \oplus 1 = 0$. However x_{856} is 0 computed using $\mathcal{D}_x f_S^4[152] \oplus x_{839} \oplus x_{846} \oplus 1$, so there is also a contradiction. Therefore, the above conditions cannot hold simultaneously that means there is no right pair following the last two DC, the 4-round forgery DC in [GPT21] is invalid as well.

5 Application to Gimli

5.1 A Brief Introduction to Gimli

Gimli [BKL+17] is one of the second-round candidates of the NIST lightweight cryptography standardization process [NIS18], including an authenticated cipher Gimli-Cipher and a hash function Gimli-Hash. Both of them are built upon the Gimli permutation that applies 24 rounds to a 384-bit state. The state of Gimli permutation is organized as a 3×4 matrix of 32-bit words denoted by $S_{i,j}, 0 \leq i < 3, 0 \leq j < 4$.The j-th column is a sequence of 96 bits such as $S_j = \{S_{0,j}, S_{1,j}, S_{2,j}\}$, the i-th row is a sequence of 128 bits such that $S_i = \{S_{i,0}, S_{i,1}, S_{i,2}, S_{i,3}\}$ (see Figure 5). In internal convention, the bits of each 32-bit word are denoted by $S[32(j + 4i) + k], 0 \leq k < 32$, where $S[\frac{32(j+4i)+k}{8}]$ indicates the least significant bit (LSB) of a byte. Each round is a sequence of three operations including a non-linear layer which is a 96-bit SP-box (SP) applied to each column, a linear mixing layer including Small-Swap (S_SW) and Big-Swap (B_SW) in every second round, and a constant addition (AC) in every fourth round. The details of components in Gimli include:

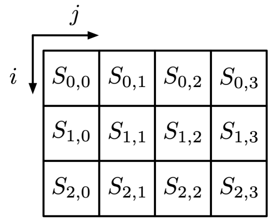

Figure 5: The matrix and indexes of the GIMLI state.

SP-boxes (SP). Each SP-box operates on each column, *i.e.*, 96 bits as follows,

$$
\begin{aligned}
x \leftarrow & S_{0,j} \lll 24 \qquad y \leftarrow S_{1,j} \lll 9 \qquad z \leftarrow S_{2,j} \\
& S_{2,j} \leftarrow x \oplus (z \ll 1) \oplus ((y \wedge z) \ll 2) \\
& S_{1,j} \leftarrow y \oplus x \oplus ((x \vee z) \ll 1) \\
& S_{0,j} \leftarrow z \oplus y \oplus ((x \wedge y) \ll 3)
\end{aligned}
$$

Small-Swap (S_SW). In the i-th round satisfying $i \bmod 4 = 0$, we apply Small-Swap operation as follows,

$$S_{0,0}, S_{0,1}, S_{0,2}, S_{0,3} \leftarrow S_{0,1}, S_{0,0}, S_{0,3}, S_{0,2}$$

Big-Swap (B_SW). In the i-th round satisfying $i \bmod 4 = 2$, we apply Big-Swap operation as follows,

$$S_{0,0}, S_{0,1}, S_{0,2}, S_{0,3} \leftarrow S_{0,2}, S_{0,3}, S_{0,0}, S_{0,1}$$

Addition of Constant (AC). When $i \in \{0, 4, 8, 12, 16, 20\}$, AC adds the round constant $\texttt{0x9e377900} \oplus (24 - i)$ to the first state word $S_{0,0}$.

Let the input state and the intermediate state after i rounds be S^i and $S^{i+1}, 0 \leq i < 24$, respectively. The 24-round GIMLI permutation can be represented with the following sequence of operations 6 times,

$$S^{4k} \xrightarrow{SP \rightarrow S\_SW \rightarrow AC} S^{4k+1} \xrightarrow{SP} S^{4k+2} \xrightarrow{SP \rightarrow B\_SW} S^{4k+3} \xrightarrow{SP} S^{4k+4}, 0 \leq k < 6.$$

In addition, the input difference and the intermediate difference after i rounds be ΔS^i and $\Delta S^{i+1}, 0 \leq i < 24$, respectively.

Gimli-Hash. The GIMLI-HASH scheme is built upon the GIMLI using a sponge construction illustrated in Figure 6. Firstly, GIMLI-Hash initializes a 48-byte GIMLI state to all-zero, then reads sequentially through a variable-length input as a series of 16-byte input blocks after padding, *i.e.*, $m_0, m_1, \ldots, m_n$. The block size is the so-called absorbing rate, *i.e.*, 128 bits. The remaining c bits of the state are called the capacity which is not directly affected by message bits, nor are they taken as output. After all message blocks are fully processed, a 32-byte hash value h can be obtained. More details of GIMLI-Hash are given in [BKL+19].

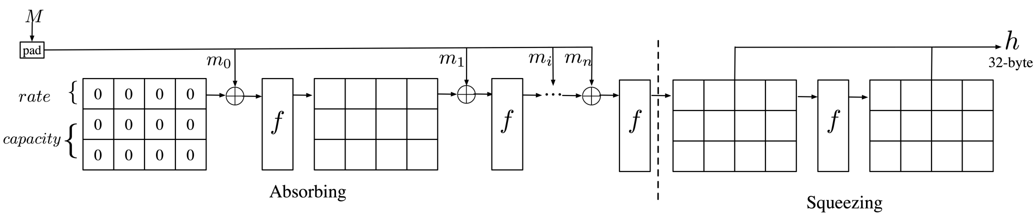

Figure 6: The illustration of the GIMLI-Hash

5.2 A Practical SFS Collision Attack on 8-Round Gimli-Hash

The Semi-Free-Start (SFS) collision attack is one of the four types of collision attacks, where the cryptanalyst can choose the initial chain value, *i.e.*, IV as well as a pair of different messages, *i.e.*, M_1, M_2 such that $H(IV, M_1) = H(IV, M_2)$ [SKP16]. For the first step of the SFS collision attack on Gimli-Hash, we need to find a special DC whose input and output differences are both active only in the rate part. In other words, we need to achieve an inner collision in the capacity part of the Gimli-Hash state. In the second step, by introducing one more pair of message blocks that has the same difference in the rate part, a real SFS collision is successfully converted.

In [LIM20], Liu *et al.* proposed an SFS collision attack on the intermediate 8 rounds of Gimli-Hash. In this attack, they firstly gave a conditional 8-round DC pattern illustrated in Figure 7. The input difference is only injected in $\Delta S^1_{0,3}$ and the difference of several internal state words is conditioned. Later, they constructed a MILP model and expect to search for a specific 8-round DC instance according to the conditional differential pattern, and make an inner collision in the capacity simultaneously. However, their MILP model is difficult to search for such an 8-round DC instance. The Gurobi solver does not output "INFEASIBLE" or any solution for an acceptable time. Thus, their SFS collision attack is in fact unsuccessful.

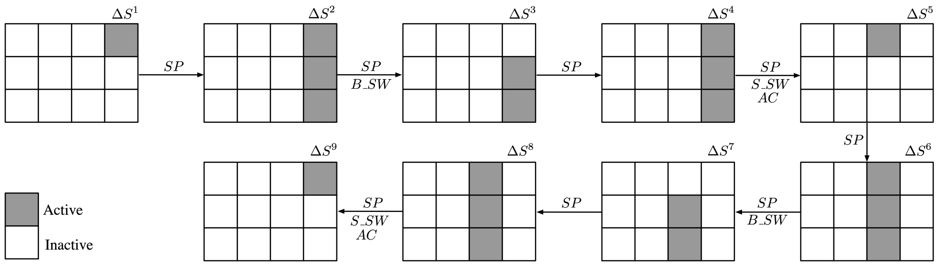

Figure 7: Semi-free-Start collision attack on the intermediate 8-round Gimli-Hash

In our attack, we aim to search for a valid 8-round DC instance according to the conditional DC in [LIM20]. Once we obtain such a valid DC as well as a right pair, we can naturally amount the SFS collision attack. Our verification algorithm introduced in Section 3 can be simply adapted for this job. Based on the given conditioned 8-round DC pattern in Figure 7, we present a SFS collision attack model shown in Figure 8.

Firstly, we let active input difference bits be free variables. In [LIM20], the difference $\Delta S^1_{0,3}$ of the conditional DC is active, which means at least one of the 32 bits of $\Delta S^1_{0,3}$ is nonzero. Therefore, in our attack model, $\Delta S^1_{0,3}$ is represented by 32 unknown binary variables, denoted by $d_0, \ldots, d_{31}$, where the rest of the difference bits of $\Delta S^1_{i,j}$ are zero. For the rest of the round difference, we only add exact ANFs of inactive bits. For example, if $\Delta S^2_{i,j} = 0$, the following 32 ANFs can be obtained

$$\mathcal{D}_x f^1_{32(j+4i)+k} = 0, 0 \le k < 32$$

where $f^1_{32(j+4i)+k}$ is the ANF of $32(j + 4i) + k$-th output bit of the first round function. Next, we take `SageMath` to generate all related ANFs that satisfy the condition of this attack model. We use `Bosphorus` to solve these ANFs. Consequently, a valid 8-round DC (see Table 9) and an inner collision (see Table 10) are successfully found at the same time. Finally, a real collision can be found by introducing one more pair of message blocks $(M, M \oplus \Delta S^9)$ to absorb the difference in the rate part. Compared with the algorithm in [LIM20], our method shows a much higher efficiency. The SAT solver returns a feasible solution in about one minute.

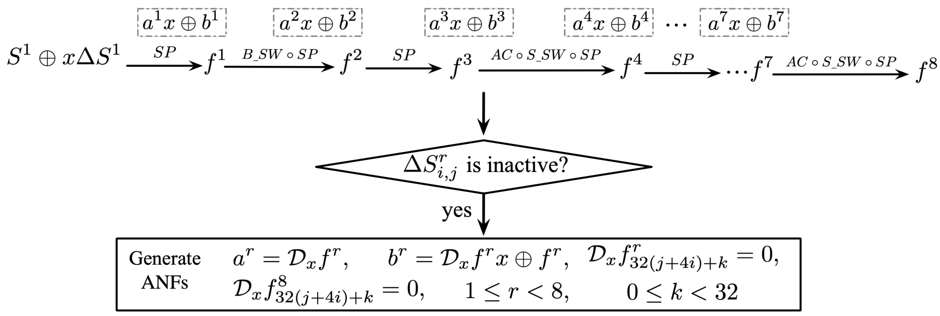

Figure 8: Our SFS collision attack model on the intermediate 8-round Gimli-Hash

Applications to 6-round Gimli-Hash. Liu *et al.* used their MILP model to search for a valid 6-round SFS collision DC according to the DC pattern in [ZDW19], which cost them about 4 hours. Our verification algorithm is more efficient than their MILP model since it took only 24.11 seconds for us to find a colliding DC (see Table 7) as well as a right pair (see Table 8) that satisfies the same DC pattern.

6 Application to Xoodoo

6.1 A Brief Introduction to Xoodoo

Xoodyak has been announced by NIST as one of ten finalists for LWC algorithms. Xoodoo presented by Daemen *et al.* [DHAK18] in ToSC 2018, is a 384-bit underlying permutation of Xoodyak, the differential nature of the former directly influences the strength of the latter against differential attacks. The state of Xoodoo is organized as a 3-dimensional array. Each bit of the array is located by (x, y, z) coordinate where $0 \leq x < 4$, $0 \leq y < 3$ and $0 \leq z < 32$. The state can be broken down into lanes or columns, or planes as shown in Figure 9.

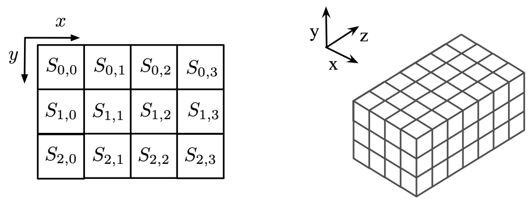

Figure 9: Illustration of the Xoodoo state (toy version)

A lane is a 32-bit word, denoted by $S_{y,x}$. A column is operated on 3 bit of y coordinate, indexed by (x, z). A plane is represented as A_y. A state is made up of 12 lanes or 128 columns or 3 planes. Similar to Gimli, in its internal convention, the bits of each 32-bit lane are denoted by $S[32(x + 4y) + z]$, where $S[\frac{32(x+4y)+z}{8}]$ indicates the LSB of a byte.

Xoodoo consists of the iteration of a round function R with 12 rounds, which has the similar design approach as Keccak-p with five step mappings *i.e.*, the linear steps θ, ρ_{west}, ι, ρ_{east}, and the non-linear step χ, denoted by $R = \rho_{east} \circ \chi \circ \iota \circ \rho_{west} \circ \theta$.

Mixing Layer θ. θ is a column parity mixer if the parity of a column is 1, we call it an *odd* (resp. *even*) column that operates as follows. Moreover, $\lll, +$ represent the logic operations rotate left, XOR, respectively.

$$P \leftarrow A_0 + A_1 + A_2 \qquad E \leftarrow P \lll (1, 5) + P \lll (1, 14)$$
$$A_y \leftarrow A_y + E \qquad \text{for } y \in \{0, 1, 2\}$$

Diffusion Layer ρ_{west} and ρ_{east}. ρ_{west} and ρ_{east} operate plane A_1 and A_2 by cyclic shift with offsets $(1,0)$ and $(0,11)$ (resp. $(0,1)$ and $(2,8)$), respectively.

$$\begin{aligned}\rho_{west}: &A_1 \leftarrow A_1 \lll (1,0) \qquad A_2 \leftarrow A_2 \lll (0,11)\\ \rho_{east}: &A_1 \leftarrow A_1 \lll (0,1) \qquad A_2 \leftarrow A_2 \lll (2,8)\end{aligned}$$

Addition of Constants ι. ι adds a constant to lane $S_{0,0}$ for each round, which is a critical step in the round function. It can be used to remove symmetry of Xoodoo state. The round constants c_i in hexadecimal notation (see Table 26), *i.e.*, the least significant bit is at $z = 0$.

Non-linear Layer χ. χ operates in parallel on 3-bit columns and as such forms a layer of 4×32 3-bit Sboxes. For 3-bit units, χ is involutive and hence this also holds for its inverse. χ has algebraic degree two and the ANF of the 3-bit Sbox is given by

$$\begin{aligned}b_0 &= a_0 \oplus (1 \oplus a_1)a_2\\ b_1 &= a_1 \oplus (1 \oplus a_2)a_0\\ b_2 &= a_2 \oplus (1 \oplus a_0)a_1\end{aligned} \tag{9}$$

6.2 Verification of the DCs for Xoodoo

In [The21], the designers updated all 3-round differential trail cores up to weight 50, and a total of 122 trail cores were found. In [BDKA21], Bordes *et al.* proved that all 3-round DCs extended from trail cores with the weight less than and equal to 50 are all valid since the differential propagations over any consecutive two rounds are independent.

However, this method is still based on some specific conditions such as the sets of input values and the sets of output values following the given differential over Sboxes are affine subspaces, while our verification algorithm is generic and does not require any such conditions.

In this section, we use our algorithm to examine these 3-round DCs again trying to find at least one right pair for each of them. Although in [BDKA21], Borders *et al.* have proved that any 3-round DCs with the weight up to 50 are valid, our verification provides interesting experimental confirmation for their theory. What's more, our algorithm presents the corresponding right pairs for the optimal DCs, which gives us more insights into the differential property of Xoodoo.

The verification algorithm for Xoodoo's DCs is basically similar to those for Ascon and Gimli, where we also need to simulate the update round function of Xoodoo.

Given an r-round DC, since the linear layers before and after the χ operations in the first and last rounds, respectively, do not influence its validity, we omit these linear layers in our verification. Consequently, r rounds of Xoodoo can be represented as

$$R^r = \chi \circ (\iota \circ \rho_{west} \circ \theta \circ \rho_{east} \circ \chi)^{r-1} = \chi \circ (\lambda \circ \chi)^{r-1}$$

where $\lambda = \iota \circ \rho_{west} \circ \theta \circ \rho_{east}$ represents the linear operation in the Xoodoo round function.

Let $(\beta_0, \alpha_1, \ldots, \alpha_r)$ be an r-round DC of Xoodoo where β_i, α_{i+1} is the input and output differences of the χ operation of the i-th round, $0 \le i < r$. Our verification process for $(\beta_0, \alpha_1, \ldots, \alpha_r)$ can be illustrated in Figure 10, where we only do $r-1$ variable substitutions.

Firstly, the input of the r-round Xoodoo is set as $X \oplus x\beta_0$, where $X = (x_0, x_1, \cdots, x_{383})$ is a 384 binary variable representing one value of the input pair, x is an auxiliary Boolean variable, and β_0 is the input difference. From the symbolic computation, we will accordingly obtain the intermediate states before and after the i-th χ, denoted by f^i and f^i_χ, respectively. Secondly, we add constraints like $\mathcal{D}_x f^i = \beta_i$ and $\mathcal{D}_x f^i_\chi = \alpha_i$ to regulate the differential transmission as our predefined DC $(\beta_0, \alpha_1, \ldots, \beta_r)$. After all, these constraints are collected

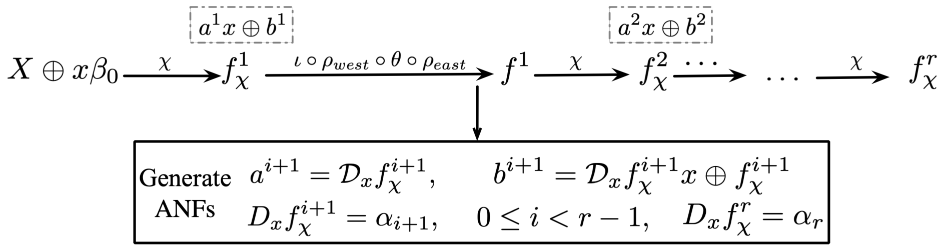

Figure 10: Verification of r-round differential trails for Xoodoo

as a SAT model. If this SAT model is solvable, a solution will be returned. $(X, X \oplus \beta_0)$ is thus a right pair for the DC. Otherwise, this DC is invalid.

As we mentioned, in [DHAK18], the designers have determined all 3-round DCs up to the weight of 50 and the four optimal DCs of weight 36. Naturally, we want to apply our verification algorithm to these DCs to check their validity. However, since the χ operation is actually 128 parallel 3-bit Sboxes and all differential propagations over these 3-bit Sboxes have the same weight, *i.e.*, 2, their search algorithm omitted the first and last χ. In other words, the weight of an r-round DC $(\beta_0, \alpha_1, \ldots, \beta_{r-1}, \beta_r)$ is totally determined by the inner state differences, *i.e.*, $(\alpha_1, \ldots, \beta_{r-1})$. $(\alpha_1, \ldots, \beta_{r-1})$ is named the *differential trail core* of $(\beta_0, \alpha_1, \ldots, \beta_{r-1}, \beta_r)$. Since every nonzero input difference of the Xoodoo 3-bit Sbox or its inverse has 4 kinds of output differences, if the input and output differences of a differential trail core activate respectively w_i and w_o Sboxes, this differential trail core can be extended at most to $2^{2(w_i+w_o)}$ DCs. It is too costly to examine all of these extended 3-round DCs, so we randomly select 2^{14} 3-round DCs from each of the four differential trail cores with the optimal weight of 36 and use our verification algorithm to check them. Finally, these 4×2^{14} 3-round DCs are all valid. This implies that the dependence between the rounds of differential propagations of Xoodoo is relatively small. Finally, our verification algorithm is not limited by the number of rounds, so we continue to check the 4-round DCs.

Similar to the 3-round cases, 4-round DC can also be determined by their differential trail core. Although the designers [DHP+20] have given the theoretical lower bound of 4-round DC with weight greater than or equal to 74 (not necessarily tight), they did not provide any concrete 4-round DCs in the literature. Recently, the authors in [DMA22] proved that the minimum weight of any 4-round differential trail core is 80.

To obtain some 4-round DC instances, we independently construct a SAT-based automatic differential trail cores search toolkit, called XoodooSat (the SAT model will be introduced later in Section D.1, as an independent interest). We successfully find two 4-round trail cores of weight 80. To apply our verification algorithm, again, we verify two 4-round DCs extended from two 4-round trail cores(see Table 35, 37), and all these two 4-round DCs are also valid. The corresponding right pairs are provided in Table 36, 38.

Applications to Keccak. Since Xoodoo and Keccak share lots of similarities, it is smooth for us to adapt the verification algorithm to examine the differentials for Keccak. We verify one 4-round DC of Keccak-f[1600] and one 4-round DC of Keccak-f[800] (see Table 8 and Table 9 in [GLST22]) with the weight of 133 and 95, respectively, and confirm that all of them are valid.

7 Conclusion

In this paper, we presented an automatic search and verification method from an algebraic perspective. Our method is handy and efficient for the target primitives with low algebraic degree round functions. We applied our approach to verify DCs the validity of Gimli, Ascon, Xoodoo, and Keccak and directly search for a valid DC of Gimli. We successfully mounted a SFS collision attack on the intermediate 8-round Gimli-Hash by searching for a valid DC as well as an inner message pair only in about one minute. We found that the published forgery attacks of Ascon-128 are invalid because the 4-round forgery characteristic in the iteration phase is invalid. Further, our verification approach could easily explain why this 4-round forgery DC is an invalid one. It is noted that our tool is not only suitable for permutations but also many other cryptographic primitives such as block ciphers, as long as the Boolean expression of the target primitives can be successfully obtained. As future works, we consider verifying longer DC and trying to apply it to other primitives. Besides, we developed a SAT-based automatic search toolkit called XoodooSat to search for the differential trail cores of any rounds and any weights. We also verify tens of thousands of 3-round DCs and two 4-round DCs extended from these differential trail cores, and find all of these DCs are valid, which well demonstrates the sound independence of the differential propagation over Xoodoo's round functions.

References

[AST+17] Ahmed Abdelkhalek, Yu Sasaki, Yosuke Todo, Mohamed Tolba, and Amr M. Youssef. MILP Modeling for (Large) S-boxes to Optimize Probability of Differential Characteristics. *IACR Trans. Symmetric Cryptol.*, 2017(4):99–129, 2017.

[BD09] Michael Brickenstein and Alexander Dreyer. PolyBoRi: A framework for Gröbner-basis computations with Boolean polynomials. *J. Symb. Comput.*, 44(9):1326–1345, 2009.

[BDKA21] Nicolas Bordes, Joan Daemen, Daniël Kuijsters, and Gilles Van Assche. Thinking Outside the Superbox. In *Advances in Cryptology - CRYPTO 2021 - 41st Annual International Cryptology Conference*, volume 12827, pages 337–367, Cham, 2021. Springer.

[BDPA11] Guido Bertoni, Joan Daemen, Michaël Peeters, and Gilles Van Assche. Duplexing the Sponge: Single-Pass Authenticated Encryption and Other Applications. In *Selected Areas in Cryptography - 18th International Workshop, SAC 2011*, volume 7118, pages 320–337, Berlin, Heidelberg, 2011. Springer.

[BDPVA07] Guido Bertoni, Joan Daemen, Michaël Peeters, and Gilles Van Assche. Sponge functions. In *ECRYPT hash workshop*, volume 2007, 2007.

[Bie19] Armin Biere. CADICAL at the SAT Race 2019. 2019. https://github.com/arminbiere/cadical.

[BKL+17] Daniel J. Bernstein, Stefan Kölbl, Stefan Lucks, Pedro Maat Costa Massolino, Florian Mendel, Kashif Nawaz, Tobias Schneider, Peter Schwabe, François-Xavier Standaert, Yosuke Todo, and Benoît Viguier. Gimli : A Cross-Platform Permutation. In *Cryptographic Hardware and Embedded Systems - CHES 2017 - 19th International Conference*, volume 10529, pages 299–320, Cham, 2017. Springer.

[BKL+19] Daniel J. Bernstein, Stefan Kölbl, Stefan Lucks, Pedro Maat Costa Massolino, Florian Mendel, Kashif Nawaz, Tobias Schneider, Peter Schwabe, François-Xavier Standaert, Yosuke Todo, and Benoît Viguier. Gimli 20190329, 2019. https://csrc.nist.gov/Projects/Lightweight-Cryptography/Round-2-Candidates.

[BM22] Emanuele Bellini and Rusydi H. Makarim. Functional Cryptanalysis: Application to reduced-round Xoodoo. *IACR Cryptol.*, 2022:134, 2022. https://eprint.iacr.org/2022/134.

[BS91] Eli Biham and Adi Shamir. Differential cryptanalysis of DES-like cryptosystems. *J. Cryptol.*, 4(1):3–72, 1991.

[CKPS00] Nicolas T. Courtois, Alexander Klimov, Jacques Patarin, and Adi Shamir. Efficient algorithms for solving overdefined systems of multivariate polynomial equations. In *Advances in Cryptology - EUROCRYPT 2000, International Conference on the Theory and Application of Cryptographic Techniques*, volume 1807, pages 392–407, Berlin, Heidelberg, 2000. Springer.

[CSCM19] Davin Choo, Mate Soos, Kian Ming Adam Chai, and Kuldeep S. Meel. Bosphorus: Bridging ANF and CNF Solvers. In *Design, Automation & Test in Europe Conference & Exhibition, DATE 2019*, pages 468–473, 2019.

[DDS12] Itai Dinur, Orr Dunkelman, and Adi Shamir. New Attacks on Keccak-224 and Keccak-256. In *Fast Software Encryption - 19th International Workshop, FSE 2012*, volume 7549, pages 442–461, Berlin, Heidelberg, 2012. Springer.

[DEMS21] Christoph Dobraunig, Maria Eichlseder, Florian Mendel, and Martin Schläffer. Ascon v1.2: Lightweight Authenticated Encryption and Hashing. *J. Cryptol.*, 34(3):33, 2021.

[DHAK18] Joan Daemen, Seth Hoffert, Gilles Van Assche, and Ronny Van Keer. The design of Xoodoo and Xoofff. *IACR Trans. Symmetric Cryptol.*, 2018(4):1–38, 2018.

[DHAK21] Joan Daemen, Seth Hoffert, Gilles Van Assche, and Ronny Van Keer. XooTools software, 2021. https://github.com/KeccakTeam/Xoodoo.

[DHP+20] Joan Daemen, Seth Hoffert, Michaël Peeters, Gilles Van Assche, and Ronny Van Keer. Xoodyak, a lightweight cryptographic scheme. *IACR Trans. Symmetric Cryptol.*, 2020(S1):60–87, 2020.

[DMA22] Joan Daemen, Silvia Mella, and Gilles Van Assche. Tighter trail bounds for Xoodoo. *IACR Cryptol.*, 2022:1088, 2022. https://eprint.iacr.org/2022/1088.

[DR02] Joan Daemen and Vincent Rijmen. *The Design of Rijndael: AES - The Advanced Encryption Standard*. Information Security and Cryptography. Springer, Berlin, Heidelberg, 2002.

[GD07] Vijay Ganesh and David L. Dill. A decision procedure for bit-vectors and arrays. In *Computer Aided Verification, 19th International Conference*, volume 4590, pages 519–531, Berlin, Heidelberg, 2007. Springer.

[GLST22] Jian Guo, Guozhen Liu, Ling Song, and Yi Tu. Exploring SAT for Cryptanalysis: (Quantum) Collision Attacks against 6-Round SHA-3. *IACR Cryptol.*, 2022:184, 2022. https://eprint.iacr.org/2022/184.

[GMS16] David Gérault, Marine Minier, and Christine Solnon. Constraint Programming Models for Chosen Key Differential Cryptanalysis. In *Principles and Practice of Constraint Programming - 22nd International Conference*, volume 9892, pages 584–601, Cham, 2016. Springer.

[GPT21] David Gérault, Thomas Peyrin, and Quan Quan Tan. Exploring Differential-Based Distinguishers and Forgeries for ASCON. *IACR Trans. Symmetric Cryptol.*, 2021(3):102–136, 2021.

[HLJ+20] Xichao Hu, Yongqiang Li, Lin Jiao, Shizhu Tian, and Mingsheng Wang. Mind the Propagation of States - New Automatic Search Tool for Impossible Differentials and Impossible Polytopic Transitions. In *Advances in Cryptology - ASIACRYPT 2020 - 26th International Conference on the Theory and Application of Cryptology and Information Security*, volume 12491, pages 415–445, Cham, 2020. Springer.

[IMM18] Alexey Ignatiev, António Morgado, and João Marques-Silva. PySAT: A Python Toolkit for Prototyping with SAT Oracles. In *Theory and Applications of Satisfiability Testing - SAT 2018 - 21st International Conference*, volume 10929, pages 428–437, Cham, 2018. Springer.

[LIM20] Fukang Liu, Takanori Isobe, and Willi Meier. Automatic Verification of Differential Characteristics: Application to Reduced Gimli. In *Advances in Cryptology - CRYPTO 2020 - 40th Annual International Cryptology Conference*, volume 12172, pages 219–248, Cham, 2020. Springer.

[LLL21] Meicheng Liu, Xiaojuan Lu, and Dongdai Lin. Differential-Linear Cryptanalysis from an Algebraic Perspective. In *Advances in Cryptology - CRYPTO 2021 - 41st Annual International Cryptology Conference*, volume 12827, pages 247–277, Cham, 2021. Springer.

[LMM91] Xuejia Lai, James L. Massey, and Sean Murphy. Markov Ciphers and Differential Cryptanalysis. In *Advances in Cryptology — EUROCRYPT '91, Workshop on the Theory and Application of of Cryptographic Techniques*, volume 547, pages 17–38, Berlin, Heidelberg, 1991. Springer.

[MLM21] João Marques-Silva, Inês Lynce, and Sharad Malik. Conflict-Driven Clause Learning SAT Solvers. In *Handbook of Satisfiability - Second Edition*, volume 336 of *Frontiers in Artificial Intelligence and Applications*, pages 133–182. IOS Press, Ohmsha, 2021.

[MP13] Nicky Mouha and Bart Preneel. Towards finding optimal differential characteristics for arx: Application to salsa20. *IACR Cryptol.*, 2013:328, 2013. https://eprint.iacr.org/2013/328.

[MWGP11] Nicky Mouha, Qingju Wang, Dawu Gu, and Bart Preneel. Differential and Linear Cryptanalysis Using Mixed-Integer Linear Programming. In *Information Security and Cryptology - 7th International Conference, Inscrypt 2011*, volume 7537, pages 57–76, Berlin, Heidelberg, 2011. Springer.

[MZ06] Ilya Mironov and Lintao Zhang. Applications of SAT Solvers to Cryptanalysis of Hash Functions. In *Theory and Applications of Satisfiability Testing - SAT 2006, 9th International Conference*, volume 4121, pages 102–115, Berlin, Heidelberg, 2006. Springer.

[NIS18] NIST. The NIST lightweight cryptography project, 2018. https://csrc.nist.gov/Projects/lightweight-cryptography.

[SHW+14] Siwei Sun, Lei Hu, Peng Wang, Kexin Qiao, Xiaoshuang Ma, and Ling Song. Automatic Security Evaluation and (Related-key) Differential Characteristic Search: Application to SIMON, PRESENT, LBlock, DES(L) and Other Bit-Oriented Block Ciphers. In *Advances in Cryptology - ASIACRYPT 2014*

- *20th International Conference on the Theory and Application of Cryptology and Information Security*, volume 8873, pages 158–178, Berlin, Heidelberg, 2014. Springer.

[Sin05] Carsten Sinz. Towards an Optimal CNF Encoding of Boolean Cardinality Constraints. In *Principles and Practice of Constraint Programming - CP 2005, 11th International Conference*, volume 3709, pages 827–831, Berlin, Heidelberg, 2005. Springer.

[SKP16] Marc Stevens, Pierre Karpman, and Thomas Peyrin. Freestart Collision for Full SHA-1. In *Advances in Cryptology - EUROCRYPT 2016 - 35th Annual International Conference on the Theory and Applications of Cryptographic Techniques*, volume 9665, pages 459–483, Berlin, Heidelberg, 2016. Springer.

[SNC09] Mate Soos, Karsten Nohl, and Claude Castelluccia. Extending SAT Solvers to Cryptographic Problems. In *Theory and Applications of Satisfiability Testing - SAT 2009*, volume 5584, pages 244–257, Berlin, Heidelberg, 2009. Springer Berlin Heidelberg.

[SRB21] Sadegh Sadeghi, Vincent Rijmen, and Nasour Bagheri. Proposing an MILP-based method for the experimental verification of difference-based trails: application to SPECK, SIMECK. *Des. Codes Cryptogr.*, 89(9):2113–2155, 2021.

[SWW18] Ling Sun, Wei Wang, and Meiqin Wang. More Accurate Differential Properties of LED64 and Midori64. *IACR Trans. Symmetric Cryptol.*, 2018(3):93–123, 2018.

[SWW21] Ling Sun, Wei Wang, and Meiqin Wang. Accelerating the Search of Differential and Linear Characteristics with the SAT Method. *IACR Trans. Symmetric Cryptol.*, 2021(1):269–315, 2021.

[The21] The Keccak Team. Updated bounds on differential and linear trails in Xoodoo, 2021. https://keccak.team/2021/updated_bounds_xoodoo.html.

[The22] The Sage Developers. *SageMath, the Sage Mathematics Software System (Version 9.5s)*, 2022. https://www.sagemath.org.

[ZDW19] Rui Zong, Xiaoyang Dong, and Xiaoyun Wang. Collision Attacks on Round-Reduced Gimli-Hash/Ascon-Xof/Ascon-Hash. *IACR Cryptol.*, 2019:1115, 2019. https://eprint.iacr.org/2019/1115.

A Detailed experimental results

To clearly illustrate the higher efficiency of our new verification method, we test the solving time in different settings with two different SAT solvers `CryptoMiniSat` and `CaDiCaL`. All the experiments in this paper are implemented on a server with Inter(R) Xeon(R) CPU E5-4650 v3 @ 2.10GHz 12 Core. The following notations are exploited to distinguish the number of ANFs , CNFs, and solving time in different cases.

- $\#\mathbf{ANF}_{Sage}$: The number of ANFs generated by `SageMath` before `Bosphorus` optimization.
- $\#\mathbf{ANF}_{Bos}$: The number of ANFs highly optimized by `Bosphorus`.
- $\#\mathbf{CNF}_{Bos}$: The number of CNFs converted by `Bosphorus`.
- $\mathbf{T}_{cms}$: Solving time using `CryptoMiniSat` with single thread by default. Note that † in here represents 20 threads we use.
- $\mathbf{T}_{cad}$: Solving time using `CaDiCaL`.

Table 3: Experimental results of Gimli

Rnd	**DC**	$\#\mathbf{ANF}_{Sage}$	$\#\mathbf{ANF}_{Bos}$	$\#\mathbf{CNF}_{Bos}$	$\mathbf{T}_{cms}$	$\mathbf{T}_{cad}$	**Pair**
6	Tab.7	6298	2916	39908	9.74s†	511s	Tab.8
8	Tab.9	8352	3734	49757	66.71s†	6454s	Tab.10

Table 4: Experimental results of Xoodoo

Rnd	**DC**	$\#\mathbf{ANF}_{Sage}$	$\#\mathbf{ANF}_{Bos}$	$\#\mathbf{CNF}_{Bos}$	$\mathbf{T}_{cms}$	$\mathbf{T}_{cad}$	**Pair**
3	Tab.27	2308	806	232984	1.37s	1.91s	Tab.28
3	Tab.29	2316	781	223258	0.12s	0.23s	Tab.29
3	Tab.31	2308	802	232384	1.62s	1.97s	Tab.32
3	Tab.33	2308	804	232517	1.08s	1.76s	Tab.34
4	Tab.35	3488	1209	425558	1.31s	2.24s	Tab.36
4	Tab.37	3464	1280	465456	343s†	28098s	Tab.38

Table 5: Experimental results of Keccak

Rnd	**DC**	$\#\mathbf{ANF}_{Sage}$	$\#\mathbf{ANF}_{Bos}$	$\#\mathbf{CNF}_{Bos}$	$\mathbf{T}_{cms}$	$\mathbf{T}_{cad}$	**Pair**
4	[GLST22] Table 8	14400	4809	4656168	21.59s†	3.52s	Tab.40
4	[GLST22] Table 9	7200	2429	2267668	7.78s†	4.44s	Tab.39

Table 6: Experimental results of Ascon

Rnd	**DC**	**#ANF**$_{Sage}$	**#ANF**$_{Bos}$	**#CNF**$_{Bos}$	**T**$_{cms}$	**T**$_{cad}$	**Pair**
2	[GPT21]	1334	465	12296	0.02s	0.02s	Tab.11
3	Tab.16	2370	707	97135	0.08s	0.12s	Tab.17
3	Tab.18	2572	1204	123651	81.98s	22.41s	Tab.19
3	Tab.12	2372	663	93695	0.07	0.11s	Tab.13
3	Tab.14	2568	835	96940	0.31s	1.20s	Tab.15
4	Tab.21	3650	1209	191994	194s†	650s	Tab.22
5	Tab.23	3265	1759	355408	3894s†	-	Tab.24

B Gimli

Table 7: The differential characteristic for SFS 6-round GIMLI-Hash

	ΔS^0		
00000000	c803ec98	00000000	c803ec98
00000000	00000000	00000000	00000000
00000000	00000000	00000000	00000000
	ΔS^1		
00000000	00000000	00000000	00000000
00000000	a9580034	00000000	a9580034
00000000	98c803ec	00000000	98c803ec
	ΔS^2		
00000000	a8c8203e	00000000	a8c8203e
00000000	a0106912	00000000	a0106912
00000000	319026b0	00000000	319026b0
	ΔS^3		
00000000	800100f0	00000000	800100f0
00000000	000ae000	00000000	000ae000
00000000	9bc00080	00000000	9bc00080
	ΔS^4		
00000000	00000080	00000000	00000080
00000000	00400000	00000000	00400000
00000000	80000000	00000000	80000000
	ΔS^5		
00000000	00000000	00000000	00000000
00000000	00000000	00000000	00000000
00000000	80000000	00000000	80000000
	ΔS^6		
00000000	80000000	00000000	80000000
00000000	00000000	00000000	00000000
00000000	00000000	00000000	00000000

Table 8: Collision message pair for SFS 6-round GIMLI-Hash

	X		
e06d07af	445efb01	1a06fc49	47fefb01
46e37879	00d119d0	807e0345	00d11880
33682fd3	03332212	7e8d4676	8334b212
	$X \oplus \Delta S^0$		
e06d07af	8c5d1799	1a06fc49	8ffd1799
46e37879	00d119d0	807e0345	00d11880
33682fd3	03332212	7e8d4676	8334b212

Table 9: The differential characteristic for intermediate 8-round GIMLI-Hash: Round 1 to 9

	ΔS^1		
00000000	00000000	00000000	81c18ba0
00000000	00000000	00000000	00000000
00000000	00000000	00000000	00000000
	ΔS^2		
00000000	00000000	00000000	00000c50
00000000	00000000	00000000	e182408d
00000000	00000000	00000000	a081c18b
	ΔS^3		
00000000	00000000	00000000	00000000
00000000	00000000	00000000	b4821adb
00000000	00000000	00000000	13068d32
	ΔS^4		
00000000	00000000	00000000	361f001b
00000000	00000000	00000000	0035a72d
00000000	00000000	00000000	3a9b6b80
	ΔS^5		
00000000	00000000	99e74180	00000000
00000000	00000000	00000000	00000000
00000000	00000000	00000000	00000000
	ΔS^6		
00000000	00000000	004c0800	00000000
00000000	00000000	808967c3	00000000
00000000	00000000	8099e741	00000000
	ΔS^7		
00000000	00000000	00000000	00000000
00000000	00000000	13ed158b	00000000
00000000	00000000	03101f8a	00000000
	ΔS^8		
00000000	00000000	186bb8bd	00000000
00000000	00000000	dc0b0437	00000000
00000000	00000000	4e8c65a4	00000000
	ΔS^9		
00000000	00000000	00000000	0806669c
00000000	00000000	00000000	00000000
00000000	00000000	00000000	00000000

Table 10: Collision message pair for intermediate 8-round GIMLI-Hash: Round 1 to 9

	X		
8e57bfca	da90441d	9134941b	3a78650c
cd0c5da0	576ee7cd	7081c41a	df260717
2a98b7a5	02fd11bb	21954066	8e042b58
	$X \oplus \Delta S^1$		
8e57bfca	da90441d	9134941b	bbb9eeac
cd0c5da0	576ee7cd	7081c41a	df260717
2a98b7a5	02fd11bb	21954066	8e042b58

C Ascon

C.1 Differential characteristics for Ascon-Hash and Conforming message pair for Forgery characteristics

Table 11: Conforming pair of 2-round differential characteristic for Ascon-Hash

DC	X	$X \oplus \beta_0$
[GPT21]	5c41069d791c645a	e70405b8a01771db
	bf65e7a5df0e6f0d	bf65e7a5df0e6f0d
	f2ced15c537c9796	f2ced15c537c9796
	36dcef2e451453f9	36dcef2e451453f9
	89b3344098ab8458	89b3344098ab8458

Table 12: Forgery characteristics for round-reduced Ascon-128A with a 3-round finalization in [GPT21]

β_0	α_1	α_2	α_3
0000000000000001	0000000000000000	0000000000000000	????????????????
0000000000000001	0000000000000000	0000000000000000	????????????????
0000000000000000	0000000000000001	8400000000000001	????????????????
0000000000000000	0000000000000000	8400000000000001	4010000000000000
0000000000000000	0000000000000000	0000000000000000	8461c20000000001

Table 13: Conforming pair of 3-round differential characteristic in Ascon-128A finalization phase [GPT21]

DC	X	$X \oplus \beta_0$
Table 12	30f78a1b80841d90	30f78a1b80841d91
	749dc43f87b6928d	749dc43f87b6928c
	a87e64223e33d3d3	a87e64223e33d3d3
	99e546e5528e8c4f	99e546e5528e8c4f
	67794a4a79d44a79	67794a4a79d44a79

Table 14: Forgery characteristics for round-reduced ASCON-128A with a 3-round permutation in [GPT21]

β_0	α_1	α_2	α_3
0040000400001004	0000000000000000	0240000402001004	2655811c3605b004
0000000000000000	0040000400001004	020080080a002024	2445011424009000
0000000000000000	0000000000000001	0000000000000000	0000000000000000
0000000000000000	0000000000000000	0000000000000000	0000000000000000
0000000000000000	0040000400001004	0a00800800002004	0000000000000000

Table 15: Conforming pair of 3-round differential characteristic in ASCON-128A permutation phase [GPT21]

DC	X	$X \oplus \beta_0$
	7c5db1d57b1562b1	7c1db1d17b1572b5
	c4ff06bf3619df87	c4ff06bf3619df87
Table 14	40078ce677be3196	40078ce677be3196
	7148974d0af4a995	7148974d0af4a995f
	6f85f592f9f630f0	6f85f592f9f630f0

Table 16: Forgery characteristics for round-reduced ASCON-128 with a 3-round finalization in [GPT21]

β_0	α_1	α_2	α_3
0000000000000001	0000000000000000	0000000000000000	????????????????
0000000000000000	0000000000000001	0200000000800000	????????????????
0000000000000000	0000000000000000	0000000002000009	????????????????
0000000000000000	0000000000000000	0000000002000008	b6010000050c0005
0000000000000000	0000000000000001	0200000000800000	0000000002008108

Table 17: Conforming pair of 3-round differential characteristic in ASCON-128 finalization phase [GPT21]

DC	X	$X \oplus \beta_0$
	df63a162860c7ade	df63a162860c7adf
	18201fba224f0c6d	18201fba224f0c6d
Table 16	a742e064fcafe921	a742e064fcafe921
	644c3786e3445133	644c3786e3445133
	06692cbc49174b50	06692cbc49174b50

Table 18: Forgery characteristics for round-reduced ASCON-128 with a 3-round permutation in [GPT21]

β_0	α_1	α_2	α_3
04000a0080014000	0000000000000000	80405826050100c0	f34a5fa78bdbc6dc
0000000000000000	04000a0080014000	054802b6010142c1	0000000000000000
0000000000000000	0000000000000000	a108588200010000	0000000000000000
0000000000000000	0000080000014000	a10858b6010142c0	0000000000000000
0000000000000000	04000a0080014000	a0081a9684034255	0000000000000000

Table 19: Conforming pair of 3-round differential characteristic in ASCON-128 iteration phase [GPT21]

DC	X	$X \oplus \beta_0$
	e3cd5bcd10216032	e7cd51cd90202032
	bed0df80d77d704a	bed0df80d77d704a
Table 18	704250acfea562a6	704250acfea562a6
	bc1556cc98493d47	bc1556cc98493d47
	404461840a57a8e8	404461840a57a8e8

Table 20: Forgery characteristics for round-reduced Ascon-128 with a 4-round permutation in [GPT21]

β_0	β_1	β_2	β_3
0000028000000000	0000000000000000	40008a4400402004	c1868824c0ca3030
0000000000000000	0000168000000005	4a00902d0280002b	8584d48c4ae22035
0000000000000000	0000000000000000	10001d5800000006	8082d4a448e20035
0000000000000000	0000000000000000	010214050a000004	40022a3085081140
0000000000000000	4000028500000001	4a8016a80800000f	0504729c47602140
β_4			
7d0b515048524344			
0000000000000000			
0000000000000000			
0000000000000000			
0000000000000000			

Table 21: Forgery characteristics for round-reduced Ascon-128 with a 4-round finalization in [GPT21]

β_0	α_1	α_2	α_3
0000000000000001	0000000000000001	0000201000000000	0200000000008000
0000000000000000	0000000000000001	0000201002000008	2000009004000000
0000000000000000	0000000000000000	0000000002000009	840120900308000d
0000000000000000	0000000000000000	0000000002000008	8605008005080005
0000000000000000	0000000000000000	0000000000000000	0200000004008100
α_4			
????????????????			
????????????????			
????????????????			
6011b00846802008			
856042820100c081			

Table 22: Conforming pair of 4-round differential characteristic in Ascon-128 finalization phase [GPT21]

DC	X	$X \oplus \beta_0$
	bd2445510dbd4c88	bd2445510dbd4c89
	5896c3af6f2ad294	5896c3af6f2ad294
Table 21	17f30c7ea871c0b0	17f30c7ea871c0b0
	e615b4b418a723b3	e615b4b418a723b3
	ce94413027760a9c	ce94413027760a9c

Table 23: The first 5 rounds differential characteristic (see Table 14-(a) in [DEMS21])

β_0	α_1	α_2	α_3
8000000000000000	0000000000000000	0000000000000000	0002000001824082
0000000000000000	8000000000000000	0100000000400000	9802a00000c64004
0000000000000000	0000000000000000	0000000001000004	1802800002c60006
0000000000000000	0000000000000000	0000000001000004	1800800002c60082
0000000000000000	8000000000000000	8100000000400000	8900200003004084
α_4	α_5		
2884024003c2a856	5a82d45841828c2a		
a4a4e8e000e0c182	c302ce434f290881		
74a062800e68cd21	1b2476214c4304cf		
1473caa04e4a3d61	9ba0b61b010c84c9		
a8f024000e847094	d2a2781b054708e6		

Table 24: Conforming pair of the first 5 rounds differential characteristic [DEMS21]

DC	X	$X \oplus \beta_0$
Table 23	f9434e1234f7d97e	79434e1234f7d97e
	acaebc0c445d988a	acaebc0c445d988a
	f5e5b6cc63c44934	f5e5b6cc63c44934
	d7c6c281c4dadfd3	d7c6c281c4dadfd3
	499d7613b65f59be	499d7613b65f59be

D Xoodoo

D.1 SAT-based Differential Trail Cores Search for Xoodoo

SAT-based automatic search has long been introduced to evaluate security bounds of cryptographic primitives. However, it's not the case of XOODOO. In this subsection, we show how to construct a SAT-based automatic search toolkit for searching XOODOO DCs called XoodooSat. The tool is used to search for differential trail cores of any rounds and any weight.

Based on this tool, we re-search for all 2- and 3-round differential trail cores whose weights are less and equal to 8 and 50, respectively, and search for all 4-round trail cores below weight 82. For 3-round XOODOO, we identify two missing trail cores of weight 48 ignored by XooTools [DHAK21] which is a search tool designed by [DHAK18]. We reported our findings to the Keccak team. They found that the missing was caused by a bug in their search code. After fixing this bug, they have confirmed that the two tools produce exactly the same set of trail cores, independently. Afterward, they extended their complete search for all 3-round trail cores of weight up to 52 [The21]. For 4-round XOODOO, we only find two trail cores of weight 80, which has been verified by our verification algorithm in Section 6.2.

D.1.1 Modeling the round function of XOODOO

An r-round DC is represented with the following form that α_i and β_i are the input differences of λ and χ, respectively. The linear layer of the round function is re-phased and defined as $\lambda = \rho_{west} \circ \theta \circ \rho_{east}$ to better describe the differential propagation properties, more details can be found in [DHAK18].

$$\alpha_0 \xrightarrow{\lambda} \beta_0 \xrightarrow{\chi} \alpha_1 \xrightarrow{\lambda} \beta_1 \xrightarrow{\chi} \alpha_2 \xrightarrow{\lambda} \beta_2 \xrightarrow{\chi} \alpha_3 \cdots \xrightarrow{\chi} \alpha_n. \tag{10}$$

The weight of n-round DC is fully determined by the sequence $\alpha_1, \ldots, \alpha_{n-1}$. Such a sequence is called a *differential trail core*. Compared to the above redundant representation of a DC, the n-round differential trail core in Equation (11) depends only on $2(n-1)$ differences. In this way, we only describe the four differences rather than six, which simplifies the generation of CNFs for our SAT problem.

$$\alpha_1 \xrightarrow{\lambda} \beta_1 \xrightarrow{\chi} \alpha_2 \xrightarrow{\lambda} \beta_2 \cdots \xrightarrow{\chi} \alpha_{n-1}. \tag{11}$$

The weight of n-round DC is given by

$$W = w(\alpha_1) + \sum_{i=1}^{n-1} w(\beta_i) \text{ or } \sum_{i=1}^{n-1} w(\alpha_i) + w(\beta_{n-1}). \tag{12}$$

Modeling the propagation properties of the linear layer. The three linear operations of the linear layer λ, *i.e.*, ρ_{east}, ρ_{west} and θ, consist of a large number of XORs. Thanks to the XOR compatibility of the solver CryptoMiniSat, we do not have to convert linear equations into CNFs.

In order to show the relationship between indexes of the input and output bits clearly, each linear operation is expressed with a $n \times n$ binary matrix M, where n is the width of XOODOO, *i.e.*, 384. Hence the XOR clauses of each input and the corresponding output bit are described through the following Equation (13).

$$\bigoplus_{j=o}^{n-1} M_{i,j} \cdot x_j \oplus y_i = 0, 0 \le i, j \le n-1 \tag{13}$$

Modeling non-linear operation. For the nonlinear layer χ, each column is treated as a 3-bit Sbox. Inspired by [AST+17, SWW18], we introduce a SAT-based method to accurately generate CNFs to describe the difference distribution table (DDT for short) of XOODOO (see Table 25).

According to the DDT, we construct a Boolean function F of $2n$-bit input, where n is the bitwise size of each input difference ($i.e.$, $a = (a_0, a_1, \ldots, a_{n-1})$) and output difference ($i.e.$, $b = (b_0, b_1, \ldots, b_{n-1})$).

$$F(a\|b) = \bigwedge_{\hat{a}\|\hat{b} \in (0,1)^{2n}} (F(\hat{a}\|\hat{b}) \vee \bigvee_{i=0}^{n-1} (a_i \oplus \hat{a}_i) \vee \bigvee_{i=0}^{n-1} (b_i \oplus \hat{b}_i)) \tag{14}$$

As shown in Equation (14) where $(\hat{a}, \hat{b})$ denotes an incompatible differential pattern, if (a, b) is a compatible differential pattern in DDT, $F(a\|b)$ returns *true*. Otherwise, it returns *false*.

In this way, 35 CNFs are generated to describe the DDT of each Sbox. An off-the-shelf software called `Logic Friday` could be introduced to further optimize these CNFs. After implementing this simplification, we only need 14 CNFs to describe the DDT.

D.1.2 Objective function

Since the weight of a difference over χ can be replaced by twice the number of active columns in XOODOO, we suppose the weight of DCs is no greater than $2N$ are searched, which is equal to the number of active columns of those 3-round trails are less and equal to N. More properties of χ refer to [DHAK18]. We introduce binary variables $AS_{i,j}$, where $0 \leq i < 3, 0 \leq j < 128$, i is the index of rounds, and j is the index of columns of a XOODOO state. If a column which is indexed by i and j is active, $AS_{i,j} = 1$. Otherwise, $AS_{i,j} = 0$.

The boolean cardinality constraint is expressed as:

$$\sum_{i=0}^{2} \sum_{j=0}^{127} AS_{ij} \leq N, \quad AS_{ij} \in \{0, 1\}.$$

The sequential encoding method proposed by Sinz in 2005 [Sin05] which has been implemented in the PySAT toolkit [IMM18] can transform the cardinality constraint into SAT problem with $O(n \cdot k)$ CNFs, where n is the number of columns and k is the maximum number of active columns.

D.1.3 Results

A SAT-based automatic search tool, called XoodooSat, is developed to generate trail cores of XOODOO. With the SAT-based tool, we verify the lower bounds on the weight of 2/3-round trail cores which are 8 and 36 respectively. As a result of independent interest, we re-search all 2/3-round trail cores up to weight 8/50.

Although the designers [DHP+20] has given the theoretical lower bound of 4-round DC with weight greater than or equal to 74, they did not provide any concrete 4-round DCs in the literature. For the exhaustive search of 4-round trail cores below weight 82, XoodooSat cannot sustain the enormous search space in a limited time (15 days). Only two trail cores of weight 80 are found (see Table 35,37). To the best of our knowledge, it is the first presented two 4-round trail cores of weight 80 in the literature.

Remark 1. With the SAT-based tool, we identify two missing trail cores of weight 48 in [DHAK18] and report to the Keccak team. They find that the missing is caused by a program bug. By fixing it, they confirm that the two tools produce exactly the same set of trail cores, independently. Afterward, they extend their complete search for all 3-round trail cores up to weight 52 [The21].

D.2 Properties of χ

Non-linear operations is a key component for generating differential and correlation weight, which leading certain input/ output difference to appear in a non-random way. χ is non-linear operation in the round function of Xoodoo as well as Keccak-p permutation. Noted that there are three differences between them. Firstly, the size of input is 3 in Xoodoo rather than 5, which can be as a 3-bit S-box. Secondly, for Xoodoo (resp. Keccak-p), χ operates on each column(resp. row) independently. Thirdly, in Xoodoo,χ is involutive due to its 3-bit input, which leads its DDT and linear approximation table(LAT) has the same weight for each possible differential as well as linear approximation.

The value of the input difference α run down the first column, while the value of output difference β run across the first row. Each valid pattern (α, β) has a non-zero value,denoted by $N_{(\alpha,\beta)}$. We can calculate the differential weight of each compatible pattern, i.e. ,$w = -log_2 \frac{N_{(\alpha,\beta)}}{8}$.

Table 25: DDT of χ operation in Xoodoo

Input	Output diff.(β)							
diff.(α)	0x0	0x1	0x2	0x3	0x4	0x5	0x6	0x07
0x0	8	0	0	0	0	0	0	0
0x1	0	2	0	2	0	2	0	2
0x2	0	0	2	2	0	0	2	2
0x3	0	2	2	0	0	2	2	0
0x4	0	0	0	0	2	2	2	2
0x5	0	2	0	2	2	0	2	0
0x6	0	0	2	2	2	2	0	0
0x7	0	2	2	0	2	0	0	2

Table 26: Constants c_i used in the Xoodoo

Round i	Constant c_i	Round i	Constant c_i	Round i	Constant c_i
-11	00000058	-7	00000120	-3	00000380
-10	00000038	-6	00000014	-2	000000f0
-9	000003c0	-5	00000060	-1	000001a0
-8	000000d0	-4	0000002c	0	00000012

D.3 Xoodoo: 3/4-round Optimal Differential characteristics and Conforming message pair

Table 27: No.1 Optimal differential characteristic for 3-round XOODOO

	β_0		
00000002	00000000	00000000	00000000
00000001	00000000	00000000	00000000
00000000	00000000	00000000	00000000
	α_1		
00000002	00000000	00000000	00000000
00000001	00000000	00000000	00000000
00000000	00000000	00000000	00000000
	α_2		
00000002	00000000	00000000	00000000
00000000	00000002	00000000	00000000
00000000	00000000	00000000	00000000
	α_3		
00000002	00008040	00010080	00000000
00000000	00000000	00008044	00010080
00000000	04020000	08040000	00000000

Table 28: Conforming pair for No.1 Optimal 3-round differential characteristic of XOODOO

	X		
da809d9d	3c7886f7	2eda462a	d60e0b26
210da579	a33b2733	c476e74e	1ce39c19
080e8bee	78a93341	f523e2b0	ff95b517
	$X \oplus \beta_0$		
da809d9f	3c7886f7	2eda462a	d60e0b26
210da579	a33b2733	c476e74e	1ce39c19
080e8bee	78a93341	f523e2b0	ff95b517

Table 29: No.2 Optimal differential characteristic for 3-round XOODOO

	β_0		
04000000	00000000	00000000	00000100
02000000	00000000	00000040	00000000
80000000	00000001	00000000	00000000
	α_1		
04000000	00000000	00000000	00000100
02000000	00000000	00000040	00000000
80000000	00000001	00000000	00000000
	α_2		
04000000	00000000	00000000	00000100
00000000	04000000	00000000	00000080
00000000	00000000	00040000	00080000
	α_3		
04000000	00000000	00000000	00000100
00000100	00000000	08000000	00000000
00000020	00000040	00000000	00000000

Table 30: Conforming pair for No.2 Optimal 3-round differential characteristic of Xoodoo

	X		
02003012	c70546a6	93480448	143ac404
80001012	00420009	41080000	20050401
04102000	c74546a6	d2401408	143fc107
	$X \oplus \beta_0$		
06003012	c70546a6	93480448	143ac504
82001012	00420009	41080040	20050401
84102000	c74546a7	d2401408	143fc107

Table 31: No.3 Optimal differential characteristic for 3-round Xoodoo

	β_0		
00000000	00000000	00000100	00000000
00000000	00000000	00000000	00000000
00000001	00000000	00000000	00000000
	α_1		
00000000	00000000	00000100	00000000
00000000	00000000	00000000	00000000
00000001	00000000	00000000	00000000
	α_2		
00000000	00000000	00000100	00000000
00000000	00000000	00000000	00000000
00000000	00000000	00080000	00000000
	α_3		
00000000	00000201	00000100	00402000
00402000	00000000	00000201	00000000
00000040	00100800	00000000	01000002

Table 32: Conforming pair for No.3 Optimal 3-round differential characteristic of Xoodoo

	X		
563794c2	088415d9	29a33b86	40abecb4
d37ced1f	ead842d6	b6782c9e	5473208f
98dfd793	087c4616	950b8157	c0f590d1
	$X \oplus \beta_0$		
563794c2	088415d9	29a33a86	40abecb4
d37ced1f	ead842d6	b6782c9e	5473208f
98dfd792	087c4616	950b8157	c0f590d1

Table 33: No.4 Optimal differential characteristic for 3-round Xoodoo

β_0			
00000000	00000000	00000000	00000000
00000000	00000000	00000080	00000000
00000001	00000000	00000000	00000000
α_1			
00000000	00000000	00000000	00000000
00000000	00000000	00000080	00000000
00000001	00000000	00000000	00000000
α_2			
00000000	00000000	00000000	00000000
00000000	00000000	00000000	00000100
00000000	00000000	00080000	00000000
α_3			
00804000	00000201	00000000	00000000
00000200	00804000	00000201	00000000
02000044	00100800	00000000	00000000

Table 34: Conforming pair for No.4 Optimal 3-round differential characteristic of Xoodoo

X			
fe518252	bd8ce600	ff7524d7	0a250b5e
ee299823	b23e3283	ecd1ba1d	6db528a5
cd66b57e	5c846c0a	11017b10	fa114ef8
$X \oplus \beta_0$			
fe518252	bd8ce600	ff7524d7	0a250b5e
ee299823	b23e3283	ecd1ba9d	6db528a5
cd66b57f	5c846c0a	11017b10	fa114ef8

Table 35: No.1 Differential characteristic for 4-round Xoodoo

β_0			
0000000e	0000000a	0000000e	0000000a
00000001	00000005	00000001	00000005
00000000	00000000	00000000	00000000
α_1			
0000000e	0000000a	0000000e	0000000a
00000007	00000005	00000007	00000005
00000000	00000000	00000000	00000000
α_2			
0000000c	0000000c	0000000c	0000000c
00000006	00000006	00000006	00000006
00000000	00000000	00000000	00000000
α_3			
00000008	00000008	00000008	00000008
00000004	00000004	00000004	00000004
00000000	00000000	00000000	00000000
α_4			
00000008	00000008	00000008	00000008
00000000	00000000	00000000	00000000
00000000	00000000	00000000	00000000

Table 36: Conforming pair for No.1 4-round differential characteristic of Xoodoo

X			
a2cd7e45	cd20443d	dc07ec29	f54c2747
7bf33691	b3816090	e7a24d70	8fa6c550
5fb494b8	76f2590a	26a4b278	bb762ada
$X \oplus \beta_0$			
a2cd7e4b	cd204437	dc07ec27	f54c274d
7bf33690	b3816095	e7a24d71	8fa6c555
5fb494b8	76f2590a	26a4b278	bb762ada

Table 37: No.2 Differential characteristic for 4-round Xoodoo

β_0			
01000100	00000000	00010001	00000000
00000000	00000000	00000000	00000000
00000000	00000000	00000000	00000000
α_1			
01000100	00000000	00010001	00000000
00000000	00000000	00000000	00000000
01000100	00000000	00010001	00000000
α_2			
01080108	00000000	08010801	00000000
00000000	00000000	00000000	00000000
01080108	00000000	08010801	00000000
α_3			
41084108	00000000	00410041	00000000
00000000	00000000	00000000	00000000
41004100	00000000	08410841	00000000
α_4			
41084108	00000000	00410041	00000000
00000000	00000000	00000000	00000000
02000200	00000000	08020802	00000000

Table 38: Conforming pair for No.2 4-round differential characteristic of Xoodoo

X			
75bb818b	566f2118	19861633	020c4018
b165f93e	007bd8f6	c2b3a741	fe8eb1b6
a52299b9	44a359d1	1c1dca29	c3f32077
$X \oplus \beta_0$			
74bb808b	566f2118	19871632	020c4018
b165f93e	007bd8f6	c2b3a741	fe8eb1b6
a52299b9	44a359d1	1c1dca29	c3f32077

E Keccak

Table 39: Conforming pair for 4-round differential characteristic of Keccak-f[800] [GLST22]

		X		
6e0afffe	fd800d8a	4022d287	b3537a30	d6b65c78
be9ede92	f5464b9a	6cedf67b	38a53a33	0ed777f9
7b0a0f76	680cd690	bba798b6	349ffde5	7e57d84a
f45f264a	41a1e30f	c9101439	a10a3fb2	07e3ba49
a532921a	611a224e	e027aa10	36804867	fc42e2e6
		$X \oplus \beta_0$		
2e0afffe	d9800d8a	4022d287	b3537a30	d6b65c78
fe9ede92	f5464b9a	4cedf67b	78a53a33	0ed777f9
3b0a0f76	680cd690	9ba798b6	349ffde5	7e57d84a
f45f264a	45a1e30f	e9101439	a10a3fb2	07e3ba49
e532921a	611a224e	c027aa10	36804867	fc42e2e6

Table 40: Conforming pair for No.1 4-round differential characteristic of Keccak-f[1600] [GLST22]

		X		
315671d0d0071602	42fd1c41f82b838b	889cdc68f9955a8a	09687aad0335ab19	22c4588ab8ff3e66
3b9e4c0062cdcfc0	5cf91c118a6b9d29	6a02da273a3c06eb	f4a05ed9a49cae3a	aec18c639c6f7a8e
0aec05b00e3d51c0	5e6993b7cab8dc03	98fea95e6a2fb529	05058568b40ea8cf	cd8777e845686eae
9b85ebd1b9ab6716	fd65f99a6f278aa0	3c55b89a8c46af0f	050fad93c11d356c	2baf07920fdec3af
dfe99de2b880f360	55e35833d55f5c2a	f5b1745d702e2291	2db565d2c98140cd	29e6612766e261d6
		$X \oplus \beta_0$		
315671d0d0071606	42fd1c41f82b838b	889cdc68f9955a8a	09687aad0335ab1b	22c4588ab8ff3e6e
3b9e4c0062cdcfc4	5cf91c118a6b9d29	6a02da273a3c06eb	f4a05ed9a49cae38	aec18c639c6f7a86
0aec05b00e3d51c4	5e6993b7cab8dc03	98fea95e6a2fb529	05058568b40ea8cd	cd8777e845686ea6
9b85ebd1b9ab6712	fd65f99a6f278aa0	2c55b89a8c46af0f	050fad93c11d356e	2baf07920fdec3af
dfe99de2b880f364	55e35833d55f5c2a	e5b1745d702e2293	2db565d2c98140cd	29e6612766e261de